

UNIVERSIDADE DE PASSO FUNDO

Eduardo dos Santos Rodrigues

**EFEITO DO DIÂMETRO DO IMPLANTE E DA
ALTURA DO PILAR NA CARGA DE FRATURA DA
CONEXÃO MORSE FRICCIONAL: TESTE IN
VITRO E ANÁLISE DE ELEMENTOS FINITOS**

Passo Fundo

2021

Eduardo dos Santos Rodrigues

**EFEITO DO DIÂMETRO DO IMPLANTE E DA
ALTURA DO PILAR NA CARGA DE FRATURA DA
CONEXÃO MORSE FRICCIONAL: TESTE IN
VITRO E ANÁLISE DE ELEMENTOS FINITOS**

Tese apresentada ao Programa de Pós-Graduação em Odontologia da Faculdade de Odontologia da UPF, para obtenção do título de Doutor em Odontologia – Área de Concentração em Clínica Odontológica, sob orientação da profa. Dra. **Maria Salete Sandini Linden** e co-orientação da profa. Dra. **Paula Benetti**.

Passo Fundo

2021

Folha reservada para
Ata de aprovação da Banca Examinadora

Observação:

Mantenha esta página no seu arquivo, imprimindo-a.
Após, faça a substituição pela Ata de aprovação fornecida pela
Secretaria para manter a correta numeração do seu trabalho.

Folha reservada para
Ficha catalográfica

Observação:

Mantenha esta página no seu arquivo, imprimindo-a.
Após, faça a substituição pela Ficha Catalográfica fornecida pela
Biblioteca Central de Estudantes da UPF para manter a correta
numeração do seu trabalho.

BIOGRAFIA DO AUTOR

Eduardo dos Santos Rodrigues

Nascido em 1º de Julho de 1982 em Passo Fundo/RS, formado em Odontologia na Universidade de Passo Fundo em 2005, especialista em Implantodontia pela Soebrás/Funorte/Elosul núcleo Passo Fundo em 2010, mestre em Clínica Odontológica pela Universidade de Passo Fundo em 2016. Atualmente, atua como professor no Técnico de Radiologia no Integrado/UPF, professor no curso Técnico de Prótese Dentária na Elosul em Passo Fundo, e atua como Implantodontista em consultório particular.

AGRADECIMENTOS

Primeiramente, gostaria de agradecer aos colegas pelos momentos de descontração e de aprendizado vividos.

Aos professores pelo aprendizado, por compartilhar o conhecimento e as experiências de vida de vocês. Agradeço principalmente às professoras Maria Salete Sandini Linden e Paula Benetti pela paciência e pelo tempo despendido me auxiliando com a minha tese.

À Universidade de Passo Fundo que forneceu a bolsa necessária para a realização do Curso de Doutorado.

Ao Antônio Carvalho da empresa Isocompósitos e à FGM, pois graças ao auxílio desses apoiadores que consegui finalizar o trabalho.

À minha esposa pela paciência e pelo apoio na realização do Doutorado, sem ela não teria chegado até aqui.

SUMÁRIO

LISTA DE TABELAS	9
LISTA DE FIGURAS.....	10
LISTA DE ABREVIATURAS.....	11
RESUMO	12
ABSTRACT	15
INTRODUÇÃO.....	17
PROPOSIÇÃO	22
ARTIGO I.	24
Introduction	27
Materials and methods	29
Results.....	33
ARTIGO II.	50
Introduction	54
Materials and methods	55
Results.....	61
Discussion	64
CONSIDERAÇÕES FINAIS	74
REFERÊNCIAS	76

LISTA DE TABELAS

<i>Table I.1 - Mechanical properties of material used for FEA.</i>	<i>32.</i>
<i>Table I.2 – Mean and standard deviation of the loading force (N).</i>	<i>34.</i>
<i>Table I.3 – Mean and standard deviation of the bending moment (Nmm).</i>	<i>34.</i>
<i>Table I.4 - Failure mode of the specimens.</i>	<i>35.</i>
<i>Table I.5 - Maximum von Mises stress (MPa).</i>	<i>36.</i>
<i>Table II.1 - Mechanical properties of material used for FEA. ...</i>	<i>48.</i>
<i>Table II.2 – Mean and standard deviation of the loading force (N).</i>	<i>50.</i>
<i>Table II.3 – Mean and standard deviation of the bending moment (Nmm).</i>	<i>51</i>
<i>Table II.4 - Failure mode of the specimens.</i>	<i>52</i>

LISTA DE FIGURAS

- Figure I.1 - Representative images of each group assembly under testing: A- Narrow diameter, 3.3mm; B – regular implant, 3.8 mm, and C- Wide implant, 4.3 mm. ...30.*
- Figure I.2 - Representative images of failure modes: A - Fracture located in the third root; B – Plastic deformation of NI platform showing the maximum stress region; C – Fracture located in the 4th root, and D – Plastic deformation of RI platform.....36.*
- Figure I.3 - Representative images of the stress distribution: A – Abutment showing in the bottom the maximum stress; B – NI group showing in the inside the maximum stress; C – RI group and D – WI group.....37.*
- Figure II.1 - Mean force load and SD (N) of the tested groups. 51.*
- Figure II.2 - Mean bending moment (Nmm) of the tested groups.52.*

LISTA DE ABREVIATURAS

mm	Milímetro
N	Newton
HE	Hexágono Externo
HI	Hexágono Interno
CMF	Cone Morse Friccional
CMPI	Cone Morse com Pilar Indexado
CMPS	Cone Morse com Pilar Sólido
ISO	International Organization for Standardization
mm/min	Milímetro por minuto
Nmm	Newton-milímetro
SMT	Screwless Morse Taper
M	Momento fletor
F	Força aplicada
CAD	Computer-Aided Design

RESUMO^a

O objetivo deste estudo busca foi avaliar a distribuição e magnitude de tensões em implantes Arcsys® de diferentes diâmetros e de pilares angulados com diferentes alturas de transmucoso, e sua capacidade de resistir a cargas compressivas. A pesquisa foi dividida em 2 artigos para poder dar enfoques diferentes à cada um dos fatores observados neste estudo, sendo eles, o diâmetro do implante e a altura do transmucoso do pilar. Dessa forma, o primeiro artigo buscou avaliar o comportamento à fratura de implantes de 3 diferentes diâmetros (3,3, 3,8 e 4,3 mm), e o segundo artigo buscou comparar os pilares com diferentes alturas de transmucoso (2,5 e 5,5 mm). Os implantes de ambos os artigos foram montados com a mesma configuração para o teste. Os espécimes foram colocados em um dispositivo que posicionou os corpos de prova em 45° e utilizando um pistão metálico de ponta plana em uma máquina universal de testes foi realizada a compressão dos conjuntos até a fratura dos corpos de prova ou até uma queda de 100 N da carga de fratura. O momento fletor foi

^a Eduardo dos Santos Rodrigues

calculado com base na ISO 14801:2016. Os dados foram estatisticamente analisados com ANOVA 1 fator e pós-teste de Tukey ($p < 0,05$). Após a falha, todos os espécimes foram observados em estereomicroscópio e foram categorizados em 3 modos de falha: fratura, deformação e intacto. No primeiro artigo, foram encontradas fraturas em todos os implantes 3,3 e 3,8, e somente deformação nos implantes 4,3. Nos pilares observou-se que os pilares dos dois primeiros grupos estavam intactos, porém no grupo mais largo foram encontradas deformações nos pilares. No segundo artigo, os pilares de diferentes alturas foram testados com implantes 4,3, pois foi o único grupo em que se encontrou deformações no pilar. No estereomicroscópio observou-se a deformação de todos os pilares de 2,5 mm de transmucoso e de 40% dos pilares de 5,5 mm de transmucoso. Na análise de elementos finitos, avaliando-se o diâmetro dos implantes com a mesma altura de pilar, observa-se que o aumento o diâmetro é proporcional à redução da concentração de tensões no sistema. Quando se avalia as diferentes alturas de transmucoso, observa-se que à medida que se aumenta a altura de transmucoso observa-se um aumento das tensões no pilar, porém essas tensões são reduzidas no implante.

Palavras-chave: implantes dentários, teste in vitro, elementos finitos, prótese dentária, titânio.

ABSTRACT^b

The aim of this study was to evaluate the distribution and magnitude of stresses in Arcsys® implants of different diameters and angled abutments with different transmucosal heights, and their ability to resist compressive loads. The research was divided into 2 articles in order to give different approaches to each of the factors observed in this study, namely, the diameter of the implant and the height of the transmucosal pillar. Thus, the first article sought to assess the fracture behavior of implants of 3 different diameters (3.3, 3.8 and 4.3 mm), and the second article sought to compare abutments with different transmucosal heights (2.5 and 5.5 mm). The implants of both articles were assembled with the same configuration for the test. The specimens were placed in a device that positioned the specimens at 45° and using a flat-tipped metallic piston in a universal testing machine, the sets were compressed until the specimens fractured or until a drop of 100 N from the fracture load. Bending moment was calculated based on

^b Effect of implant diameter and abutment height on frictional morse connection fracture load: in vitro test and finite element analysis

ISO 14801:2016. Data were statistically analyzed with 1-way ANOVA and Tukey's post-test ($p < 0.05$). After failure, all specimens were observed under a stereomicroscope and were categorized into 3 failure modes: fracture, deformation, and intact. In the first article, fractures were found in all implants 3.3 and 3.8, and only deformation in implants 4.3. In the columns, it was observed that the columns of the first two groups were intact, but in the wider group, deformations were found in the columns. In the second article, abutments of different heights were tested with implants 4,3, as this was the only group in which deformations in the abutment were found. Under the stereomicroscope, deformation of all 2.5 mm transmucosal pillars and 40% of the 5.5 mm transmucosal pillars were observed. In finite element analysis, evaluating the diameter of implants with the same abutment height, it is observed that the increase in diameter is proportional to the reduction in the concentration of stresses in the system. When evaluating the different heights of the transmucosal, it is observed that as the height of the transmucosal increases, there is an increase in tensions in the abutment, but these tensions are reduced in the implant.

Keywords: dental implants, in vitro test, finite elements, dental prosthesis, titanium.

INTRODUÇÃO

A colocação dos implantes dentais para reabilitação com próteses implantossuportadas tem se tornado cada vez mais frequente no Brasil, de forma que, cerca de 800 mil implantes são colocados e 2,4 milhões de componentes são utilizados ao ano no país (1). Por isso o desenvolvimento de materiais mais resistentes e conexões mais estáveis são essenciais para durabilidade a longo prazo no tratamento com implantes (2,3).

Desde o desenvolvimento dos implantes dentários endósseos diversas inovações foram realizadas, tanto na sua superfície, para reduzir o tempo de osseointegração (4), como na conexão com a coroa protética para melhorar a resistência biomecânica (5). Dentre elas é possível citar, desenvolvimento de conexões implante/pilar mais estáveis, mudanças do diâmetro e comprimento dos implantes dentários, utilização de novas ligas metálicas e utilização de ligas cerâmicas, mudanças nas características micro e macrogeométricas dos implantes (2,6,7).

As frequentes inovações na implantodontia torna complexa a escolha do sistema de implante/conexão mais apropriado, pois a

utilização de novas metodologias nem sempre resultam em melhores resultados clínicos a longo prazo (8). Dessa forma, é necessária a compreensão do desempenho dos sistemas de implantes dentários para que sejam alcançadas altas taxas de sucesso nas reabilitações.

Dentre as inovações na conexão implante-pilar, o cone Morse (CM) mostrou uma maior manutenção dos tecidos periimplantares a longo prazo quando comparado com os sistemas Hexágono Interno (HI) e Hexágono Externo (HE) (9–11), possivelmente devido aos melhores resultados de formação de *microgap* e selamento bacteriano do CM comparado com os outros sistemas (9). A transferência das tensões para os tecidos circundantes quando as cargas são aplicadas axialmente é semelhante entre os sistemas (10), porém, quando é utilizada a plataforma switching menores valores na distribuição de estresses para a região periimplantar são encontradas (12,13).

Mecanicamente, a maioria dos estudos encontrou resultados favoráveis ao CM (3,9,14–16), enquanto alguns encontraram resultados favoráveis ao HE (17,18). Nos diferentes sistemas de implante diversos fatores podem influenciar no afrouxamento do pilar/parafuso protético que, conseqüentemente, podem ocasionar a deformação do parafuso do pilar ou mesmo do implante. Estes fatores podem estar relacionados ao parafusos protético: como força de pré-carga e valor de torque de apertamento, repetidos

ciclos de apertamento e afrouxamento do parafuso, desenho das roscas, material, diâmetro e comprimento do pescoço do parafuso; ou relacionados ao implante: sistema de implante, liga de titânio, posicionamento do implante; ou até mesmo relacionados ao pilar: material do pilar, adaptação do pilar ao implante, falhas na fabricação do pilar e da coroa protética, altura e angulação do pilar (19).

Falha mecânica é considerada tanto o afrouxamento do parafuso protético/pilar como a fratura do parafuso/pilar/implante. As falhas mecânicas encontradas no implante CM estão relacionadas principalmente à fina espessura das paredes da plataforma em implantes estreitos (20), à espessura das paredes da plataforma do componente em contato com o implante quando é utilizado o parafuso passante e ao fino diâmetro do parafuso passante utilizado (21). A fratura de implantes e/ou componentes protéticos é uma situação clínica de resolução complexa (22–27) que pode levar, em algumas situações, à inutilização ou remoção do implante (28,29), por isso, a escolha inadequada das características do implante ou do componente pode fazer com que a longevidade clínica do tratamento seja comprometida.

Como a falha mecânica dos implantes CM ocorre na maioria das vezes no parafuso protético começou-se a utilizar o cone Morse sem parafuso (friccional), em que, utilizando-se de um martelete, o pilar é ativado sobre o implante proporcionando um aumento de

atrito entre as superfícies, gerando o fenômeno de solda fria. Para competir no mercado nacional de implantes dentários, em 2016, o Sistema Arcsys® (FGM, Joiville, Brasil) chegou ao mercado brasileiro utilizando o cone Morse Friccional (CMF) associado aos implantes estreitos. Nesta configuração, o implante dentário foi fabricado com liga de titânio grau 5 e os componentes fabricados com a liga de aço inoxidável ASTM F138-13a (30).

Estudos clínicos com CMF relatam ausência de fratura de implantes ou pilares, ausência de afrouxamento de pilares em próteses parciais fixas múltiplas e próteses fixas de arco completo, e baixa ocorrência de afrouxamento em coroas protéticas unitárias (entre 0,37%, a 0,65% em um tempo de avaliação entre 4 anos e 10 anos) (31). Em acompanhamento do desempenho de implantes estreitos (diâmetro de 3,3mm) por 10 anos foi encontrado o afrouxamento 0,3% dos pilares (32). Com relação aos implantes curtos, os implantes de comprimento de 8 mm apresentaram 0,45% pilares sofreram afrouxamento em em 10 anos (33), e de comprimento de 6,5mm (implantes extra-curtos) 1,5% dos pilares afrouxaram em 5 anos (34). Em carga imediata, 5% dos pilares (3/57 implantes) afrouxaram em 2 anos de acompanhamento (35), e 0,5% (3/594 pilares) em 11 anos (36). Todos os pilares frouxos encontrados nos estudos foram recolocados e não voltaram a soltar.

Em um estudo clínico, 20 pacientes foram reabilitados com overdentures suportadas por dois implantes dentários (4mm de

diâmetro e 12 mm de comprimento) na região de caninos inferiores, sendo colocado um implante CMF de um lado e no outro lado um implante cone Morse com pilar indexado (CMPI) e parafuso protético. Após 1 ano de acompanhamento não foi encontrada fratura ou afrouxamento de nenhum dos implantes/componentes, não sendo encontradas diferenças estatisticamente significantes nos resultados mecânicos e biológicos (37).

A literatura é incipiente quanto à avaliação da influência do diâmetro do implante e da altura do transmucoso na distribuição de tensões e desempenho mecânico de cone-morse friccional. Por este motivo, este estudo busca analisar a distribuição e magnitude de tensões em implantes Arcsys® de diferentes diâmetros e de pilares angulados com diferentes alturas de transmucoso, e sua capacidade de resistir à cargas compressivas.

PROPOSIÇÃO

1 Objetivo geral

Avaliar a carga máxima de fratura, a distribuição e a magnitude de tensões no sistema cone Morse friccional em diferentes configurações de diâmetro de implante e altura de pilar, por meio de carregamento monotônico e análise de elementos finitos.

2 Objetivos específicos

- A. Avaliar e comparar a distribuição de tensões no conjunto implante e pilar em diferentes configurações, utilizando a aplicação de carga não-axial em análise de elementos finitos (*in silico*).
- B. Comparar a carga de fratura de conjuntos de implantes cone Morse de diferentes diâmetros (3,3; 3,8 e 4,3) e pilares angulados em 20° com 2 diferentes alturas de transmucoso (2,5 e 5,5 mm) em teste de carregamento não-axial monotônico.
- C. Avaliar em estereomicroscópio o modo de falha das diferentes configurações do sistema e compará-las com as áreas de

concentração de tensões encontradas na simulação em elementos finitos.

Hipóteses testadas:

- Hipótese 1 - diferentes configurações de implante e pilar não interfere a distribuição e magnitude de tensões.
- Hipótese 2 - diâmetro do implante não interfere na carga de fratura do sistema.
- Hipótese 3 - altura do transmucoso do componente não interfere na carga de fratura do sistema.
- Hipótese 4 – o modo de falha será similar entre as diferentes configurações implante e pilar.

**ARTIGO A SER SUBMETIDO AO THE JOURNAL
OF PROSTHETIC DENTISTRY**

ARTIGO I.

**LOAD-BEARING CAPACITY AND STRESS
ANALYSIS OF SCREWLESS MORSE TAPER
IMPLANTS WITH DIFFERENT DIAMETERS**

**Eduardo dos Santos Rodrigues, DDS, MSc^a, Maria S. S.
Linden, DDS, MSc, PhD^b, Paula Benetti, DDS, MSc, PhD^c**

Corresponding author:

Paula Benetti

Campus I, BR 285, CEP 99001-970

Tel.: +55 54 33168402

email: paulabenetti@upf.br

^a Doctoral student, Post-Graduate Program in Dentistry, Dental School, University of Passo Fundo, Rio Grande do Sul, Brazil.

^b Professor of Implantology, Post-Graduate Program in Dentistry, Dental School, University of Passo Fundo, Rio Grande do Sul, Brazil.

^c Professor of Prosthodontics, Post-Graduate Program in Dentistry, Dental School, University of Passo Fundo, Rio Grande do Sul, Brazil.

Abstract

Statement of a problem: foldable abutment simplifies the rehabilitation with angled implants. However, while different implant diameter would interfere in the mechanical behavior of the system is unclear. Purpose: the aim of this study was to compare the load bearing capacity of screwless implants of different diameters using compressive monotonic testing and in silico analysis.

Materials and methods: Arcsys (FGM) morse taper implants (n=10) were selected with 13 mm in length and 3 diameters: narrow implant (NI – 3.3mm), regular implant (RI – 3.8mm) and wide implant (WI – 4.3 mm). Screwless abutments were attached to the implant and folded at 20°. Hemispherical zirconia caps were placed over the abutments. In the monotonic compressive test (ISO 14801:2016), the load was applied at 45° (moment arm) and crosshead speed of 0.5 mm/min until implant/abutment fracture or load drop of 100 N. Mean load at fracture of the groups was compared using One-way ANOVA and Tukey post-hoc test (5% significance). Finite element analysis (FEA) was designed as the compressive strength test, however the tested force was 170 N for all groups. The stress distribution was analyzed with von Mises stress.

Results: Significant differences on failure load were found between the groups ($p < 0.05$). The WI demonstrated higher fracture load and

bending moment than the other groups, while the NI had the lowest fracture loads and bending moment. In FEA, it was observed that the increase in the implant diameter is proportional to the stress distribution reduction in the assembly.

Conclusion. Wide implants showed higher load-bearing capacity and lower implant fractures than narrower implants.

Keywords: dental implants, dental implant-abutment design, compressive strength, finite element analysis.

CLINICAL IMPLICATIONS

Using wider implants is advantageous to the mechanical performance of the implant-abutment assembly, since they support higher loads without fractures and favors the deformation of the abutment, which, in the clinical situation results simply on the prosthetic component and prosthesis replacement.

Introduction

The number of rehabilitations using implants can reach 23% of American adults treated in 2026 (1). Biologic and technical complications are frequently reported for implant-supported crowns after 5 years of function, such as bone loss (7%), fracture of veneering material (6.5%), loss of retention (4.3%), abutment screw loosening (2.1%) and abutment fracture (0.4%) (2). Several innovations have been made in dental implants to improve the performance of these rehabilitations (3,4), such as the development of more stable implant / abutment connections, changes in the diameter of dental implants and the use of new metal alloys (5–7).

Among the implant systems used today, the Morse taper implant is more favorable for peri-implant tissues (8,9) and fatigue studies have found favorable results for the Morse taper implants comparing to other connections (9–12), while some have found favorable results for the external connection (13,14).

The choice of the most appropriate implant system is difficult (15). The improper characteristics of the implant or the abutment can compromised the clinical longevity of the treatment by biological or mechanical complications (16–18). The mechanical failures found in the Morse taper implant are mainly related to the thin thickness of the platform walls in narrow implants (19), the thickness of the abutment in contact with the

implant when using abutment screw, and the thin diameter of the screw (20). Implant fracture can be related to implant diameter, location in the mouth and parafunctional habits (grinding/bruxism). As narrow implants are frequently used in anterior and pre-molars region, they suffer higher stresses than molars region due to off axis (lateral) forces (16). The fracture of implants and/or prosthetic components is a clinical situation of complex solving (21–26) that can lead, in some situations, to the need for implant removal (27,28). For this reason, the development of stronger materials and more stable connections are essential for long-term durability in implant treatment. (6,11).

In 2016, the Arcsys® System (FGM, Joinville, Brazil) reached the Brazilian market using the Screwless Morse taper (SMT) associated to narrow implants. The grade 5 titanium alloy was used for the dental implant and the ASTM F138-13a stainless steel alloy was used for the components (29). The stability of SMT connection is possible due to the large contact pressure and resulting frictional resistance, also called tapered interference fit, eliminating the problems that arise from abutment screws (30,31).

Mechanical complications (abutment loosening or abutment/implant fracture) are found in SMT implants. The loosening of the abutment in single crowns have being reported in literature ranging from 0.3% to 1.5% (32–38), while some studies find no loose abutment (39–42). Increased crown-to-implant length

ratio on single tooth implants have a significant effect in the loosening of maxillary anterior abutments, and fracture of 2 mm diameter abutments in posterior region (43).

Finite element analysis (FEA) is an adequate method to simulate the stress distribution in the implant/abutment connection and to predict where the plastic deformation or fracture can occur (44–47). This analysis can improve the understanding of the stress behavior SMT implants of different diameters when the abutment is activated and occlusal forces are applied (48).

Hence, this study compared the mechanical behavior of SMT implants with different diameters mounted with angulated abutments using compressive monotonic test and *in silico* analysis. The tested hypothesis is that the diameter of the implant has no influence on the stress distribution and load-bearing capacity of the system.

Materials and methods

SMT implants (n=30) (Arcsys, FGM, Joinville, SC, Brazil) of 13 mm length with three different diameters (3.3 mm, 3.8 mm and 4.3 mm) were obtained for this study. An isophthalic glass fiber-reinforced resin-based composite (20 mm length x 19 mm diameter), which has an elastic modulus of approximately 13 GPa (49), was used as bone analog (50). Arcsys drills for each implant diameter were used to obtain a perforation of 10 mm deep in each

block. The implants were screwed in the perforation leaving 3 mm of their surface uncovered by the analog, to simulate a bone loss situation.

Foldable abutments (n=30, Arcsys®, FGM) (2.5 mm transmucosal height x 6 mm height x 4.2 mm width) were assembled to the implants, producing 3 groups (Figure I.1) according to the implant diameter (n=10): narrow (NI), regular (RI) and wide implant (WI). All foldable abutments were folded at 20° with Arcsys abutment folding device to test the components in the worst condition. Abutments were placed in the implants and activated three times with abutment placement tool as recommended by manufacturers. Custom hemispherical zirconia caps were placed over the abutments to simulate the implant-supported crowns.

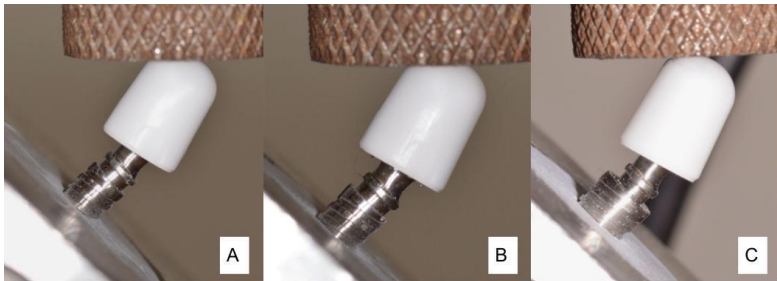


Figure I.1 – Representative images of each group assembly under testing: A- Narrow diameter, 3.3mm; B – regular implant, 3.8 mm, and C- Wide implant, 4.3 mm.

The samples were placed in 45° off-axis loading device as most implant fractures happens in anterior region (16). The

compressive monotonic test was performed according to the ISO 14801:2007 (51). The load was applied by a metal flat piston in a universal testing machine (Instron, model 2310, São José dos Pinhais, Brazil) at a crosshead speed of 0.5 mm/min until failure. Failure was defined as fracture of implant/abutment connection, or a force drop of 100 N. The maximum loading force (F , in N) was recorded.

The moment arm was defined as $l \times \text{sen } 45^\circ$, which l was defined as 11 mm. The bending moment was calculated by the equation $M = l \times \text{sen } 45^\circ \times F$ (52) and was reported in Nmm. Shapiro-Wilk's normality test ($P = 0.147$) and Levene's homogeneity test ($P = 0.087$) was performed for ultimate failure load and bending moment results showing that the data were normally distributed. One-way ANOVA and Tukey post-hoc test ($p < 0.05$) were performed using SigmaPlot 11.0 (Systat Software, Chicago, IL, USA).

After failure, the specimens were analyzed in binocular stereomicroscope (Zeiss, STEMI 2000-C) at 40 x magnification. Implant and abutment failure modes were categorized as fracture, deformation or intact, which was considered the implants or abutments that had no visible plastic deformation, crack or fracture in the stereomicroscopic evaluation.

In addition, computer-aided design (CAD) models of holder block, implants, abutments and cap were created using

SolidWorks® 2017 (Dassault Systèmes, SolidWorks Corps., USA) through a number of relevant measurements of the components with digital caliper (Starret). Same groups of the compressive testing were assembled in the 3D software. The length of implant and the dimensions of abutment, bone block and hemispherical cap were constant in all models. The length of implant was 13 mm and the dimension of abutment was 2.5 transmucosal height x 6 mm height x 4.2 mm width. The implant models were virtually implanted in the cylinder block with 20 mm length and 19 mm diameter.

CAD models were exported to the finite element analysis software Ansys Workbench 15.0 (Ansys Inc., Canonsburg, PA, USA) and the structures for analysis were considered isotropic, homogeneous, and linearly elastic. The material considered for each component was: isophthalic glass fiber-reinforced resin-based composite for the holder block, titanium grade 5 (Ti 6Al 4V Eli) for implant, ASTM F138 for abutment and zirconia for hemispherical loading cap. The properties of the materials are reported in Table I.1 (46,49,53,54).

Table 0.1 - Mechanical properties of material used for FEA.

Component/material	Young's Modulus (GPa)	Poisson Ratio
Holder Block (Isophthalic)	13.11	0.44

Implant (Ti G5)	114	0.33
Abutment (ASTM F138)	187.5	0.33
Loading cap (Zirconia)	200	0.31

A nonlinear analysis was conducted assuming that the contact between loading cap - abutment were bonded, also between holder block – implant to simulate complete osseointegration. A frictional contact of 0.3 (54) was considered between the inner surface of implant and outer surface of abutment. Moreover, a cylindrical support was added to the outer face of the block. The element type was tetrahedral element with four nodes for all the components. The mesh was refined in the contact areas and a convergence study with 5% was employed to validate the finite element model (55). The total number of elements in the analyzed models ranged from 120021 to 157762 and the total number of nodes ranged from 182936 to 236319.

To comprehend the behavior of the stress distribution in implant/abutment connection a force load of 170 N (56) was applied to the hemispherical cap with a 45° inclination to the long axis of the implant. The implants and abutments were analyzed according to the equivalent Von Mises stress analyses.

Results

The means and the standard deviations (SD) of the loading force for each experimental group are shown in Table I.2. A difference between the groups was found ($p = <0.001$). The group WI presented the highest failure loads, while the group NI presented the lowest value.

Table 0.2 – Mean and standard deviation of the loading force (N).

Groups	n	Mean \pm SD (N)*
NI	10	478.189 \pm 48.53 ^C
RI	10	720.897 \pm 36.65 ^B
WI	10	857.810 \pm 74.15 ^A

*Different letter in the same column indicates statistical differences between the groups ($p < 0.05$)

The means and the standard deviations (SD) of the bending moment are shown in Table I.3 and in Figure I.2. There was statistically difference between all groups ($p = <0.001$). The group NI had the lowest value when compared to other groups, and the group WI had the highest bending moment.

Table 0.3 – Mean and standard deviation of the bending moment (Nmm).

Groups	N	Mean \pm SD (Nmm)
NI	10	3,734.65 \pm 379.05 ^C

RI	10	5,630.20 ± 286.24 ^B
WI	10	6,699.49 ± 579.18 ^A

*Different letter in the same column indicates statistical differences between the groups (p < 0.05)

The frequency of observed failure modes is presented in Table I.4. Images representing each mode of failure observed in the study are presented in Figure I.2. In the stereomicroscopic evaluation, it was observed that all narrow and regular implants had plastic deformation followed by fracture after compressive strength test. All plastic deformations occurred in the inner edge of the implant platform in the direction of the applied force. Most implant fractures were located in the third root of the screw thread in the opposite side of the deformed platform. The plastic deformation observed in the implants of WI group was smaller than in the other groups. All abutments in narrow and regular implants groups were intact, while all abutments in the wide implant group had deformation in the abutment neck.

Table 0.4 - Failure mode of the specimens.

		Fracture	Deformation	Intact
NI	Implant	10	-	-
	Abutment	-	-	10
RI	Implant	10	-	-
	Abutment	-	-	10

WI	Implant	-	10	-
	Abutment	-	10	-

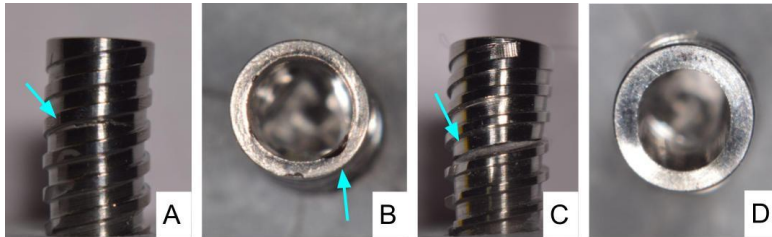


Figure I.2 – Representative images of failure modes: A - Fracture located in the third root; B – Plastic deformation of NI platform showing the maximum stress region; C – Fracture located in the 4th root, and D – Plastic deformation of RI platform.

The numerical study results (Table I.5) were proportionally compared with titanium grade 5 ultimate tensile strength of 1190 MPa (57) and stainless steel tensile strength at break of 2200 MPa (58).

Table 0.5 -Maximum von Mises stress (MPa).

	Implant	Abutment
NI	4474,9	6546,8
RI	4268	6227,1
WI	3986,7	5199,2

The qualitative results of the implants and abutments tested models shows the von Mises stress distribution with red representing the highest stress value, followed by yellow, green and blue for lowest values (Figure I.3). Under the same loading conditions, the stress distribution of the models were similar showing that the maximum stress was located in the abutment neck followed by the implant platform in all models.

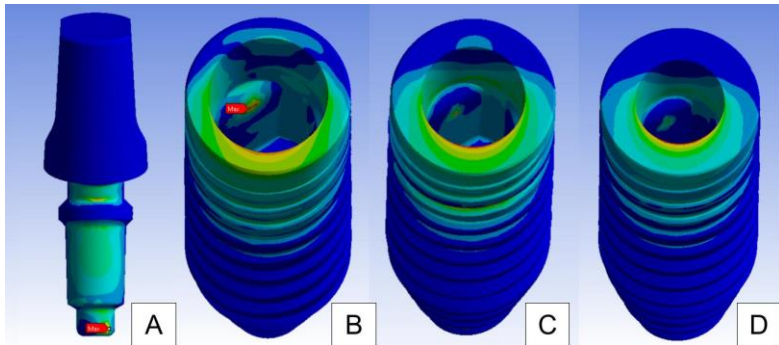


Figure I.3 – Representative images of the stress distribution: A – Abutment showing in the bottom the maximum stress; B – NI group showing in the inside the maximum stress; C – RI group and D – WI group.

Discussion

The results of this study showed that the load-bearing capacity is improved with the increase on the implants diameter, rejecting the study hypothesis. This result agrees with the literature

that also demonstrate higher fracture loads and bending moment of zirconia-implant assemblies with 4.0 mm to 4.5 mm implant platform, compared to 3.1 mm to 3.5 mm platforms. The size of the implant plays a major role in improving its strength, but the use of wide implants is difficult due to the bone thickness (59). As the bone width is often critical, an option is the use of 3.1 mm diameter implants, which has no statistical difference when compared to narrower implants as mini-implants (2.8 and 2.3 mm diameter), but has significant difference when compared to regular implant (4.1 mm diameter) (60).

A study compared the deformations in the collar of Kopp® frictional implants with diameters of 4.3 mm and 5.5 mm, and CMPI Neodent® implants of 3.5 mm and 5 mm after compression with load of 100 N. Greater deformations was found in the collars of smaller diameter Neodent implants (41). In the present study, in addition to deformation, implants with a smaller diameter presented fracture of the implant body in the contact area with the abutment. In addition to the diameter size of the implant, the stress is distributed by the screwless connection, reducing the deformation in the wide implants.

Another study compared the load-bearing capacity of different implants (4.3 mm x 13 mm): Morse taper with solid abutment (CMPS) and internal hexagon (HI) with indexed abutment and screw. The maximum force values were higher in

Morse taper implants, which presented no fractures, but permanent deformations in the implant platform and in the abutment neck (42), corroborating the findings of the present study for the largest diameter implant group (WI).

In a published finite element analysis, the stress distribution of extra-short CMF implants (Arcsys®, FGM) was evaluated using Ti-6Al-4V alloy for the implant and stainless steel for the abutment. The maximum stresses were concentrated on the inner edge of the implant platform in contact with the conical surface of the abutment, followed by the stresses located in the cone of the abutment (43). In this study it's possible to observe the same peak stress in the implant platform, however as the abutments were angulated for compressive testing there was a peak stress in the neck of the abutment where it's folded.

Using wider implants is advantageous to the mechanical performance of the implant-abutment assembly, since they support higher loads without fractures and favors the deformation of the abutment, which, in the clinical situation results simply on the prosthetic component and prosthesis replacement.

In Finite Element Analysis (FEA) favorable stress distribution in the cortical bone region were found in 5.0 mm diameter implant comparing to 3.75 mm implant (61) independently of connection type (62)(63), even when compared with traditional Morse taper implants (64). However, due to the

presence of stainless steel in Arcsys® abutments, high stress concentration can be found at the implants (54), resulting on the implant fractures observed in the present study.

The maximum voluntary bite force in the first molar region can vary from 508 N to 978 N, and the bruxism force in the same region can vary from 153 N to 796 N (65). Therefore, placing small-diameter implant in this critical area could result in fracture of the implant or permanent deformation of both implants and abutment.

The finite element method has been used in dentistry to achieve greater understanding of biomechanical behavior and need to be carefully extrapolated to clinical settings (23). Thus, when combined with well-designed clinical studies, the results of the current study could guide new strategies for addressing challenges associated with managing stress distribution in implant dentistry. However, the results should be interpreted with caution due to limitations such as factors related to the methodology, computer simulation and linearity elastic analysis, which consider bone tissue to be isotropic and homogenous and apply static occlusal loading (24,25). Therefore, additional controlled and randomized clinical studies should be conducted in order to fully explore and evaluate the clinical implications of various biomechanical parameters in implant dentistry. Within the limitation of this study can conclude that the increase in diameter was favorable for

improved stress distribution in the cortical bone region, regardless of the connection type. Morse taper implants were associated with lower stress concentration than other connections, especially during off-axis loading.

References

1. Elani HW, Starr JR, Da Silva JD, Gallucci GO. Trends in Dental Implant Use in the U.S., 1999-2016, and Projections to 2026. *J Dent Res*. 2018 Dec;97(13):1424–30.
2. Tey VHS, Phillips R, Tan K. Five-year retrospective study on success, survival and incidence of complications of single crowns supported by dental implants. *Clin Oral Implants Res*. 2017 May;28(5):620–5.
3. Coelho PG, Granjeiro JM, Romanos GE, Suzuki M, Silva NRF, Cardaropoli G, et al. Basic research methods and current trends of dental implant surfaces. *J Biomed Mater Res B Appl Biomater*. 2009;88B(2):579–96.
4. Abraham CM. A Brief Historical Perspective on Dental Implants, Their Surface Coatings and Treatments. *Open Dent J*. 2014 May 16;8:50–5.
5. Gaviria L, Salcido JP, Guda T, Ong JL. Current trends in dental implants. *J Korean Assoc Oral Maxillofac Surg*. 2014;40(2):50.
6. Duraccio D, Mussano F, Faga MG. Biomaterials for dental implants: current and future trends. *J Mater Sci*. 2015 Jul;50(14):4779–812.

7. Barbosa TP, Naves MM, Menezes HHM, Pinto PHC, Mello JDB, Costa HL. Topography and surface energy of dental implants: a methodological approach. *J Braz Soc Mech Sci Eng.* 2017 Jan 3;6(39):1895–907.
8. Caricasulo R, Malchiodi L, Ghensi P, Fantozzi G, Cucchi A. The influence of implant-abutment connection to peri-implant bone loss: A systematic review and meta-analysis. *Clin Implant Dent Relat Res.* 2018 Aug;20(4):653–64.
9. Schmitt CM, Nogueira-Filho G, Tenenbaum HC, Lai JY, Brito C, Döring H, et al. Performance of conical abutment (Morse Taper) connection implants: A systematic review: Performance of Conical Implant-Abutment Connection Systems. *J Biomed Mater Res A.* 2014 Feb;102(2):552–74.
10. Freitas G, Hirata R, Bonfante E, Tovar N, Coelho P. Survival Probability of Narrow and Standard-Diameter Implants with Different Implant-Abutment Connection Designs. *Int J Prosthodont.* 2016 Feb;29(2):179–85.
11. Pjetursson BE, Zarauz, C., Stranding, M., Sailer, I, Zwahlen, M., Zembic, A. A systematic review of the influence of the implant-abutment connection on the clinical outcomes of ceramic and metal implant abutments supporting fixed implant reconstructions. *Clin Oral Implants Res.* 2018;29(18):160–83.
12. Tsuruta K, Ayukawa Y, Matsuzaki T, Kihara M, Koyano K. The influence of implant–abutment connection on the screw loosening and microleakage. *Int J Implant Dent* [Internet]. 2018 Dec [cited 2018 Oct 10];4(1). Available from: <https://journalimplantdent.springeropen.com/articles/10.1186/s40729-018-0121-y>
13. Ribeiro CG, Maia MLC, Scherrer SS, Cardoso AC, Wiskott HWA. Resistance of three implant-abutment interfaces to

- fatigue testing. *J Appl Oral Sci Rev FOB*. 2011 Aug;19(4):413–20.
14. Seol H-W, Heo S-J, Koak J-Y, Kim S-K, Han C-H. Effect of cyclic loading on axial displacement of abutment into implant with internal tapered connection: a pilot study. *J Korean Acad Prosthodont*. 2013;51(4):315.
 15. Lee J-H, Frias V, Lee K-W, Wright RF. Effect of implant size and shape on implant success rates: A literature review. *J Prosthet Dent*. 2005;94(4):377–81.
 16. Chrcanovic BR, Kisch J, Albrektsson T, Wennerberg A. Factors influencing the fracture of dental implants. *Clin Implant Dent Relat Res*. 2018;20(1):58–67.
 17. Stoichkov B, Kirov D. Analysis of the causes of dental implant fracture: A retrospective clinical study. *Quintessence Int*. 2018 Mar 16;49(4):279–86.
 18. Stoicănescu M, Buzamet E, Budei DV, Craciun V, Budei R, Cosnita M, et al. Possible Causes in Breaking of Dental Implants Research. *Mater Sci Forum*. 2017 Sep;907:104–18.
 19. Singh A, Singh A, Vivek R, Chaturvedi TP, Chauhan P, Gupta S. SEM Analysis and Management of Fracture Dental Implant. *Case Rep Dent*. 2013;2013:270385.
 20. Lee J-H, Lee J-B, Kim M-Y, Yoon J-H, Choi S-H, Kim Y-T. Mechanical and biological complication rates of the modified lateral-screw-retained implant prosthesis in the posterior region: an alternative to the conventional Implant prosthetic system. *J Adv Prosthodont*. 2016 Apr;8(2):150–7.
 21. Imam AY, Yilmaz B, Özçelik TB, McGlumphy E. Salvaging an angled implant abutment with damaged internal threads: A clinical report. *J Prosthet Dent*. 2013;109(5):287–90.

22. Imam AY, Moshaverinia A, Chee WWL, McGlumphy EA. A technique for retrieving fractured implant screws. *J Prosthet Dent.* 2014;111(1):81–3.
23. Canpolat C, Özkurt-Kayahan Z, Kazazoğlu E. Management of a Fractured Implant Abutment Screw: A Clinical Report: Fractured Abutment Screw. *J Prosthodont.* 2014 Jul;23(5):402–5.
24. Yilmaz B, Mascarenhas F. Salvaging an implant with damaged internal threads. *J Prosthet Dent.* 2015;114(2):301–4.
25. Carneiro T de APN, Prudente MS, e Pessoa RS, Mendonça G, das Neves FD. A conservative approach to retrieve a fractured abutment screw – Case report. *J Prosthodont Res.* 2016 Apr;60(2):138–42.
26. Oh S-L, Barnes D. Managing a fractured implant: A clinical report. *J Prosthet Dent.* 2016 Apr;115(4):397–401.
27. Muroff FI. Removal and Replacement of a Fractured Dental Implant: Case Report: *Implant Dent.* 2003 Sep;12(3):206–10.
28. AL Quran FAM, Rashan BA, AL-Dwairi ZN. Management of Dental Implant Fractures. A Case History. *J Oral Implantol.* 2009 Aug;35(4):210–4.
29. Mittelstadt FG, Wiggers W, Cecato RC. Perfil técnico implante Arcsys [Internet]. DENTSCARE LTDA; 2016 [cited 2019 Mar 17]. Available from: https://issuu.com/fgmprodutosodontologicos/docs/arcsys_perfil_tecnico_final_rev01_v
30. Bozkaya D, Müftü S. Mechanics of the tapered interference fit in dental implants. *J Biomech.* 2003 Nov;36(11):1649–58.

31. Ugurel CS, Steiner M, Isik-Ozkol G, Kutay O, Kern M. Mechanical resistance of screwless morse taper and screw-retained implant-abutment connections. *Clin Oral Implants Res.* 2013;26(2):137–42.
32. Mangano F, Lucchina AG, Bruccoli M, Migliario M, Mortellaro C, Mangano C. Prosthetic Complications Affecting Single-Tooth Morse-Taper Connection Implants: *J Craniofac Surg.* 2018 Mar;1.
33. Mangano C, Mangano F, Piattelli A, Iezzi G, Mangano A, La Colla L. Prospective clinical evaluation of 1920 Morse taper connection implants: results after 4 years of functional loading. *Clin Oral Implants Res.* 2009 Mar;20(3):254–61.
34. Mangano C, Mangano F, Shibli JA, Tettamanti L, Figliuzzi M, d'Avila S, et al. Prospective Evaluation of 2,549 Morse Taper Connection Implants: 1- to 6-Year Data. *J Periodontol.* 2011;82(1):52–61.
35. Mangano F, Macchi A, Caprioglio A, Sammons RL, Piattelli A, Mangano C. Survival and Complication Rates of Fixed Restorations Supported by Locking-Taper Implants: A Prospective Study with 1 to 10 Years of Follow-Up. *J Prosthodont.* 2014;23(6):434–44.
36. Mangano F, Shibli JA, Sammons RL, Veronesi G, Piattelli A, Mangano C. Clinical Outcome of Narrow-Diameter (3.3-mm) Locking-Taper Implants: A Prospective Study with 1 to 10 Years of Follow-up. *Int J Oral Maxillofac Implants.* 2014;29(2):448–55.
37. Mangano FG, Shibli JA, Sammons RL, Iaculli F, Piattelli A, Mangano C. Short (8-mm) locking-taper implants supporting single crowns in posterior region: a prospective clinical study with 1-to 10-years of follow-up. *Clin Oral Implants Res.* 2014;25(8):933–40.

38. Mangano F, Frezzato I, Frezzato A, Veronesi G, Mortellaro C, Mangano C. The Effect of Crown-to-Implant Ratio on the Clinical Performance of Extra-Short Locking-Taper Implants: *J Craniofac Surg*. 2016 May;27(3):675–81.
39. Demiralp KÖ, Akbulut N, Kursun S, Argun D, Bagis N, Orhan K. Survival Rate of Short, Locking Taper Implants with a Plateau Design: A 5-Year Retrospective Study. *BioMed Res Int* [Internet]. 2015 [cited 2019 Mar 28]; Available from: <https://www.hindawi.com/journals/bmri/2015/197451/>
40. Geckili E, Geckili O, Bilhan H, Kutay O, Bilgin T. Clinical Comparison of Screw-Retained and Screwless Morse Taper Implant-Abutment Connections: One-year Postloading Results. *Int J Oral Maxillofac Implants*. 2017 Sep;32(5):1123–31.
41. Mangano C, Luongo F, Mangano FG, Macchi A, Perrotti V, Piattelli A. Wide-diameter locking-taper implants: a prospective clinical study with 1 to 10-year follow-up. *J Osseointegration*. 2014 Jun 30;6(2):28–36.
42. Urdaneta RA, Daher S, Leary J, Emanuel KM, Chuang S-K. The Survival of Ultrashort Locking-Taper Implants. 2012;12.
43. Urdaneta RA, Rodriguez S, McNeil DC, Weed M, Chuang S-K. The effect of increased crown-to-implant ratio on single-tooth locking-taper implants. *Int J Oral Maxillofac Implants*. 2010 Jul 1;25(4):729–43.
44. Rodrigues EDS, Benetti P, Carli JPD, Paranhos LR, Santos PL, Linden MS. A Comparison of Torque Stress on Abutment Screw of External Hexagon and Morse Taper Implant. *J Contemp Dent Pract*. 2018 Nov 1;19(11):1306–11.

45. Petris GP, De Carli JP, Paranhos LR, Santos PL, Benetti P, Walber M, et al. Morse taper performance: A finite element analysis study. *Clinics* [Internet]. 2019 Mar 25 [cited 2021 Jun 20];74. Available from: <https://www.scielo.br/j/clin/a/YnmswGQRbJRcTBVthVDpNGs/?lang=en>
46. de la Rosa Castolo G, Guevara Perez SV, Arnoux P-J, Badih L, Bonnet F, Behr M. Mechanical strength and fracture point of a dental implant under certification conditions: A numerical approach by finite element analysis. *J Prosthet Dent*. 2018 Apr;119(4):611–9.
47. Erdemir A, Guess TM, Halloran J, Tadepalli SC, Morrison TM. Considerations for reporting finite element analysis studies in biomechanics. *J Biomech*. 2012 Feb;45(4):625–33.
48. Chang H-C, Chang C-H, Li H-Y, Wang C-H. Biomechanical analysis of the press-fit effect in a conical Morse taper implant system by using an in vitro experimental test and finite element analysis. *J Prosthet Dent*. 2020 Dec;S0022391320306934.
49. Merlo EG, Della Bona A, Griggs JA, Jodha KS, Corazza PH. Mechanical behavior and adhesive potential of glass fiber-reinforced resin-based composites for use as dentin analogues. *Am J Dent*. 2020 Dec;33(6):310–4.
50. Verplancke K, Waele WD, Bruyn HD. DENTAL IMPLANTS, WHAT SHOULD BE KNOWN BEFORE STARTING AN IN VITRO STUDY. 2011;10.
51. International Organization for Standardization. ISO 14801:2007 Dentistry — Implants — Dynamic fatigue test for endosseous dental implants. Geneva, Switzerland; 2007.

52. Santos VT de G, Trento CL, Santos PRS, Siqueira A dos S, Santos SV dos, Griza S. Análise da resistência à fratura entre pilares retos e angulados do sistema cone Morse. *Rev Odontol UNESP*. 2015 Apr;44(2):67–73.
53. Wu Y-L, Tsai M-H, Chen H-S, Chang Y-T, Lin T-T, Wu AY-J. Biomechanical effects of original equipment manufacturer and aftermarket abutment screws in zirconia abutment on dental implant assembly. *Sci Rep*. 2020 Dec;10(1):18406.
54. de Souza Rendohl E, Brandt WC. Stress distribution with extra-short implants in an angled frictional system: A finite element analysis study. *J Prosthet Dent*. 2020 Dec;124(6):728.e1-728.e9.
55. Chang H-C, Li H-Y, Chen Y-N, Chang C-H, Wang C-H. Mechanical analysis of a dental implant system under 3 contact conditions and with 2 mechanical factors. *J Prosthet Dent*. 2019 Oct;122(4):376–82.
56. Kawaguchi T, Kawata T, Kuriyagawa T, Sasaki K. In vivo 3-dimensional measurement of the force exerted on a tooth during clenching. *J Biomech*. 2007 Jan 1;40(2):244–51.
57. Proto Labs Titanium Grade 5 Ti-6Al-4V - DMLS [Internet]. [cited 2021 Jun 30]. Available from: <http://www.matweb.com/search/DataSheet.aspx?MatGUID=12529329832a4a0295dbf5451b8c4c75&ckck=1>
58. Medical Grade Stainless Steel 316LVM [Internet]. [cited 2021 Jun 30]. Available from: <http://www.matweb.com/search/DataSheet.aspx?MatGUID=29a84d10fada4e4fa3ebe3986e52d848>
59. Saker S, AL-Zordk W, Özcan M. Resistance to Fracture of Zirconia Abutments with Different Angulations: Impact of

- Implant Platform Diameter. *Eur J Dent.* 2020 Oct;14(04):517–24.
60. Song S-Y, Lee J-Y, Shin S-W. Effect of Implant Diameter on Fatigue Strength. *Implant Dent.* 2017 Feb;26(1):59–65.
 61. Pellizzer EP, Verri FR, Falcón-Antenucci RM, Júnior JFS, de Carvalho PSP, de Moraes SLD, et al. Stress Analysis in Platform-Switching Implants: A 3-Dimensional Finite Element Study. *J Oral Implantol.* 2012 Oct 20;38(5):587–94.
 62. Moraes SLD de, Verri FR, Santiago Júnior JF, Almeida DA de F, Lemos CAA, Gomes JM de L, et al. Three-Dimensional Finite Element Analysis of Varying Diameter and Connection Type in Implants with High Crown-Implant Ratio. *Braz Dent J.* 2018 Feb;29(1):36–42.
 63. Sannino G, Barlattani A. Mechanical Evaluation of an Implant-Abutment Self-Locking Taper Connection: Finite Element Analysis and Experimental Tests. *Int J Oral Maxillofac Implants.* 2013;28(1):e17–26.
 64. Markose J, Suresh S, Eshwar S, Rekha K, Jain V, Manvi S. Comparison of Platform Switched and Sloping Shoulder Implants on Stress Reduction in various Bone Densities: Finite Element Analysis. *J Contemp Dent Pract.* 2017 Jun 1;18(6):510–5.
 65. Nishigawa K, Bando E, Nakano M. Quantitative study of bite force during sleep associated bruxism. *J Oral Rehabil.* 2001 May;28(5):485–91.

**ARTIGO II.
INFLUENCE OF TRANSMUCOSAL HEIGHT ON
THE MECHANICAL BEHAVIOR OF FRICTIONAL
IMPLANT SYSTEM: IN VITRO AND IN SILICO
ANALYSIS**

**Eduardo dos Santos Rodrigues, DDS, MSc^a, Maria S. S.
Linden, DDS, MSc, PhD^b, Paula Benetti, DDS, MSc, PhD^c**

Corresponding author:

Paula Benetti

Campus I, BR 285, CEP 99001-970

Tel.: +55 54 33168402

email: paulabenetti@upf.br

^a Doctoral student, Post-Graduate Program in Dentistry, Dental School, University of Passo Fundo, Rio Grande do Sul, Brazil.

^b Professor of Implantology, Post-Graduate Program in Dentistry, Dental School, University of Passo Fundo, Rio Grande do Sul, Brazil.

^c Professor of Prosthodontics, Post-Graduate Program in Dentistry, Dental School, University of Passo Fundo, Rio Grande do Sul, Brazil.

Abstract

Statement of the problem: foldable abutment of different transmucosal length increases the rehabilitation possibilities when an angled implant and different mucosa thickness is present. However, whether the abutment length contributes or not to the hole implant system behavior is not elucidated in the literature.

Purpose: the aim of this study was to investigate the effect of screwless foldable abutments with different transmucosal heights on the fracture load, mode of failure and stress distribution of morse taper abutment-implants system.

Materials and methods: Arcsys (FGM) screwless morse taper implants (n=20) with 4.3 mm width x 13 mm length were divided into 2 groups (n=10) according to the transmucosal height: short abutment (WS, 2.5 mm) and long abutment (WL, 5.5 mm). The abutments attached to the implant were folded at 20°. Na hemispherical zirconia cap was placed on the abutment. The assemblies were submitted to a monotonic compressive test following the ISO 14801:2016. A gradual load (0.5 mm/min) was applied at 45° (moment arm) until implant/abutment failure (fracture or load drop of 100 N). Groups were compared using One-way ANOVA and Tukey post-hoc test (5% significance). Finite element analysis (FEA) was designed as the compressive strength test, however the tested force was 170 N for all groups. The stress distribution was analyzed with von Mises stress.

Results: Significant differences on failure load and bending moment were found between the groups ($p < 0.05$). It was found higher fracture load in the WS group, however, in the bending moment calculation the WL group presented higher values. In FEA, it was observed that the increase in the transmucosal height is proportional to the stress distribution reduction in the implant, however there was an increase in the maximum stress of the abutment.

Conclusion. Short transmucosal height abutment showed higher load-bearing capacity, however, long transmucosal height abutments presented higher bending moment. The increase of transmucosal height presented better stress distribution to the implant, however there was an increase in the maximum stress to the abutment.

Keywords: dental implants, dental implant-abutment design, compressive strength, finite element analysis.

CLINICAL IMPLICATIONS

Using long transmucosal height associated to stainless steel abutment is advantageous to the mechanical performance of the implant-abutment assembly, since the steel supports higher loads without fractures and bring a protective effect to the assembly, reducing the probability of deformation of the abutment and the

implant. The use of foldable abutment is a secure option to adjust the angulation of the abutment.

Introduction

The fracture of implants or prosthetic components is a clinical situation of complex resolution (1–6) that can result in the abutment or, in some cases, in the removal of the implant (7,8). For this reason, the development of alternative types of connections are essential for the longevity of the rehabilitation with implant-supported prosthesis (9,10).

The Arcsys® System (FGM, Joinville, Brazil) is a Screwless Morse taper (SMT), made of grade 5 titanium alloy, that are compatible with stainless steel alloy foldable abutments available in different transmucosal height to fulfill the requirements of the presented clinical situation, such as angled implants, mucosa of different thickness and heights (11).

The clinical studies sought in the literature that analyzed the mechanical complications (abutment loosening or abutment/implant fracture) in SMT implants report few failures in this type of connection, the most common complication was loosening of the abutment in single crowns that ranged from 0.3% to 1.5% (12–18), all the prosthetic abutments were reinserted and no further loosening was observed during the observation period. Some studies didn't find any loose abutment (19–22). No abutment or implant fracture was found in the clinical studies.

Increasing the collar height also increases the crown-to-implant ratio (C:I), which can increase the marginal bone loss (23)

and potentially influences the mechanical behavior of the implant-abutment assembly. A study evaluated loosening of the prosthetic screw under fatigue testing different transmucosal heights (0.8, 3.5 e 5.5 mm), finding no statistically difference between the groups (24). Foldable abutments are a suitable and safe option to modify the abutment angulation to place the prosthesis in the correct position, without the costs of keeping a large stock of different components (25,26).

In Finite Element Analysis (FEA) favorable stress distribution were found in SMT implants (27), even when compared with traditional Morse taper implants (28). However, due to the presence of stainless steel in Arcsys® abutments, this can lead to high stress concentration at the implant (29).

Therefore, the aim of this study is to investigate the effect of screwless foldable abutments with different transmucosal heights on the fracture load, mode of failure and stress distribution of morse taper abutment-implants system, testing the hypothesis that the length of the abutment has no influence on the mechanical behavior of the system.

Materials and methods

A total of 20 foldable abutments with two different transmucosal height (2.5 mm and 5.5 mm) were assembled in 20 SMT implants (Arcsys, FGM, Joinville, SC, Brazil) of 4.3 mm

width x 13 mm length, resulting in two experimental groups (n = 10): short abutment (WS) and long abutment (WL).

Most procedures involving the sample assembly to the compressive test was performed according to ISO 14801:2007 (30). The stabilization of the assembly at 45° off-axis loading (31) was the only adaptation of the ISO to test the implants with the incisal guide angle (32), as most implant fractures happens in anterior region (33). Implants were placed in a 20 mm length x 19 mm diameter isophthalic glass fiber-reinforced resin-based composite which has an elastic modulus of approximately 13 GPa (34) serving well as “bone-like” analog (35). Arcsys drills for each diameter were used for perforation at 10 mm deep in each block. Implants were screwed until it had 3 mm of implant surface uncovered to simulate bone loss condition.

All foldable abutments for cement-retained restoration (Arcsys®, FGM) were folded at 20° with Arcsys abutment folding device to test the components in the worst condition. Abutments were placed in the implants and activated three times with abutment placement tool as recommended by manufacturers. Custom zirconia hemispherical loading members were placed over the abutments to be tested in the maximum compressive strength test (Figure II.1).

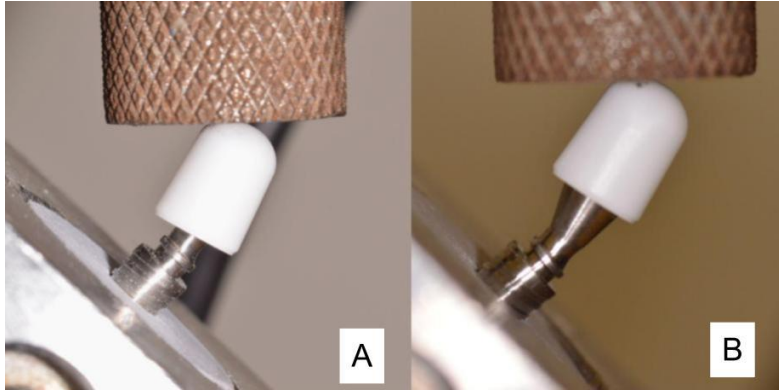


Figure II.1 – Representative images of each group assembly under testing: A- short abutment; B – long abutment

The compressive strength test was performed with a metal rod in a universal testing machine (Instron, model 2310, São José dos Pinhais, Brazil) with a load cell of 10 kN and crosshead speed of 0.5 mm/min. The loading force (F) was applied to the specimens until failure, which was defined as fracture of implant/abutment connection or a force drop of 100 N. The maximum load required to fracture or to deform the components was recorded in Newtons.

The moment arm was defined as $l \times \sin 45^\circ$. For specimens with 2.5 mm transmucosal height abutment l was defined as 11 mm, and for 5.5 mm specimens it was 14 mm. The bending moment was calculated by the equation $M = l \times \sin 45^\circ \times F$ (36) and was reported in Nmm. Shapiro-Wilk's normality test ($P = 0.147$) and Levene's homogeneity test ($P = 0.087$) was performed for ultimate failure load and bending moment results showing that

the data were normally distributed. One-way ANOVA and Tukey post-hoc test ($p < 0.05$) were performed using SigmaPlot 11.0 (Systat Software, Chicago, IL, USA).

In the compressive strength test the ultimate failure load was recorded and the bending moment was determined. Shapiro-Wilk's normality test ($P = 0.456$) and Levene's homogeneity test ($P = 0.083$) was performed for compressive strength and for bending moment ($P = 0.816$ and $P = 0.220$) showing that the data were normally distributed. One-way ANOVA and Tukey post-hoc test ($p < 0.05$) were performed for both results using SigmaPlot 11.0 (Systat Software, Chicago, IL, USA).

After failure, the specimens were separated and were analyzed in binocular stereomicroscope (Zeiss, STEMI 2000-C) at 40 x magnification. Implant and abutment failure modes were categorized as fracture, deformation or intact, which was considered the implants or abutments that had no visible deformation, crack or fracture in the stereomicroscope.

In addition, computer-aided design (CAD) models of holder block, implants, abutments and cap were created using SolidWorks® 2017 (Dassault Systèmes, SolidWorks Corps., USA) through a number of relevant measurements of the components with digital caliper (Starret). Same groups of the compressive testing were assembled in the 3D software.

CAD models were exported to the finite element analysis software Ansys Workbench 15.0 (Ansys Inc., Canonsburg, PA, USA) and the structures for analysis were considered to be isotropic, homogeneous, and linearly elastic. The material considered for each component was: isophthalic glass fiber-reinforced resin-based composite for the holder block, titanium grade 5 (Ti 6Al 4V Eli) for implant, ASTM F138 for abutment and zirconia for hemispherical loading cap. The properties of the materials are reported in Table II.1 (29,34,37,38).

Table 10.1 - Mechanical properties of material used for FEA.

Component/material	Young's Modulus (GPa)	Poisson Ratio
Holder Block (Isophthalic)	13.11	0.44
Implant (Ti G5)	114	0.33
Abutment (ASTM F138)	187.5	0.33
Loading cap (Zirconia)	200	0.31

The length of implant and the dimensions of abutment and the bone block were constant in all models. The length of implant was 10 mm and the dimension of abutment was 6 x 4.2 mm and the cylinder block were 20 x 20 mm. A nonlinear analysis was conducted assuming that the contact between loading cap - abutment were bonded, also between holder block – implant to

simulate complete osseointegration. A frictional contact of 0.36(39) was considered between the inner surface of implant and outer surface of abutment. Moreover, the mesial and distal edges of the cortical shell were fixed. The element type was C3D4 (tetrahedral element with four nodes) for all the components. The mesh was refined in the contact areas and a convergence study was employed to validate the finite element model. The total number of elements in the analyzed models ranged from 280,180 to 333610 and the total number of nodes ranged from 398539 to 469385 (Figure II.2).

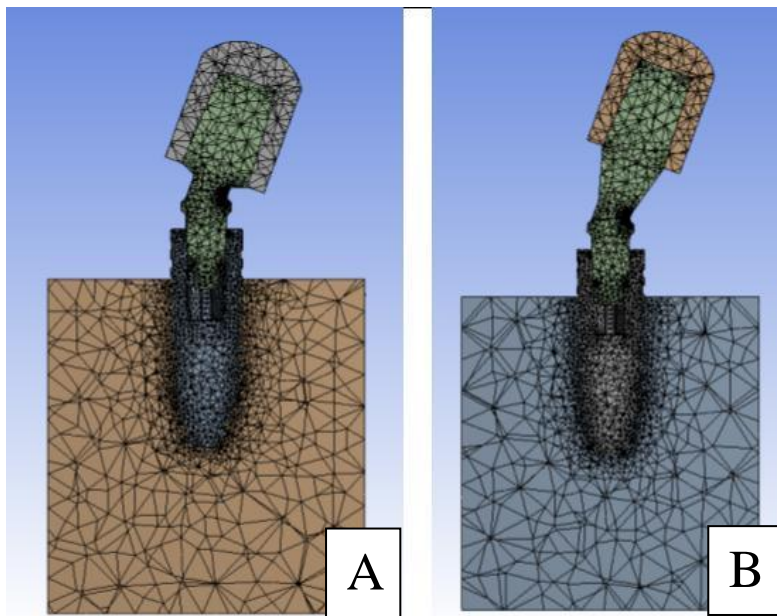


Figure II.2 – Images of mesh convergence: A- Group WS and B – group WL.

To comprehend the behavior of the stress distribution in implant/abutment connection a force load of 170 N (40) was applied to the hemispherical cap with a 45° inclination to the long axis of the implant. The implants and abutments were analyzed according to the equivalent Von Mises stress analyses.

Results

The means and the standard deviations (SD) of the maximum load registered for experimental groups are shown in Table II.2. There was a statistical difference between WS and WL. plants with 2.5 mm transmucosal height abutments had higher failure loads than implants with 5.5 mm abutments

Table 10.2 – Mean and standard deviation of the loading force (N) of the experimental groups.

Groups	n	Mean ± SD (N)*
WS	10	857.810 ± 74.15 ^A
WL	10	767.933 ± 45.49 ^B

* Different letter in the same column shows statistical differences (p < 0.05).

The means and the standard deviations (SD) of the bending moment in the compressive test are shown in Table II.3. Implants with 5.5 mm transmucosal height abutments had higher bending moment than implants with 2.5 mm abutments.

Table 10.3 – Mean and standard deviation of the bending moment (Nmm).

Groups	N	Mean ± SD (Nmm)
WS	10	6,699.49 ± 579.18 ^B
WL	10	7,633.25 ± 452.24 ^A

*Values followed by different letter in the same column are statistically different (p < 0.05)

The frequency of observed failure modes is presented in Table II.4. Images representing each mode of failure observed in the study are presented in Figure II.2. In the stereomicroscopic evaluation, it was observed that all implants had plastic deformation in the inner edge of the implant platform in the direction of the applied force. The plastic deformation observed in the implants of WL group was smaller than in the WS group. Deformation of the abutments neck was the most frequent failure observed in both groups.

Table 10.4 - Failure mode of the specimens according to the experimental group.

		Fracture	Deformation	Intact
WS	Implant	-	10	-
	Abutment	-	10	-
WL	Implant	-	10	-

	Abutment	-	4	6
--	----------	---	---	---

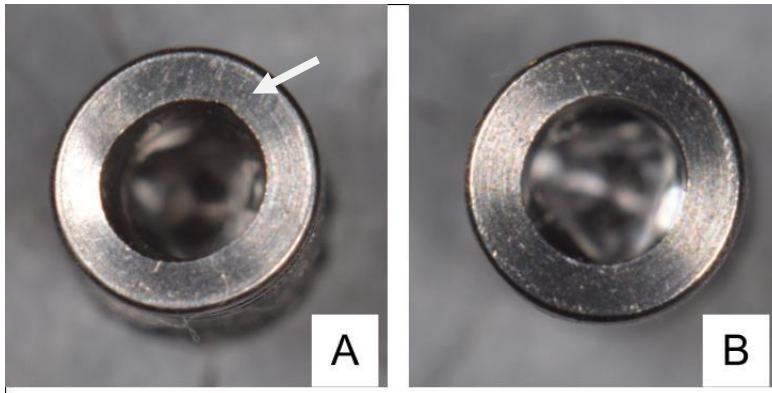


Figure I.3 – Representative images of failure modes: A - Plastic deformation of the WS group showing the stress concentration in the platform; B – Plastic deformation of the WL platform.

The numerical study results (Table I.5) were proportionally compared with titanium grade 5 ultimate tensile strength of 1190 MPa (41) and stainless steel tensile strength at break of 2200 MPa (42).

Table 0.5 -Maximum von Mises stress (MPa).

	Implant	Abutment
WS	4811,3	6165,2
WL	4119,3	8250,3

The qualitative results of the implants and abutments tested models shows the von Mises stress distribution with red

representing the highest stress value, followed by yellow, green and blue for lowest values (Figure II.4). Under the same loading conditions, the stress distribution of the models was similar showing that the maximum stress was located in the abutment neck followed by the implant platform in all models.

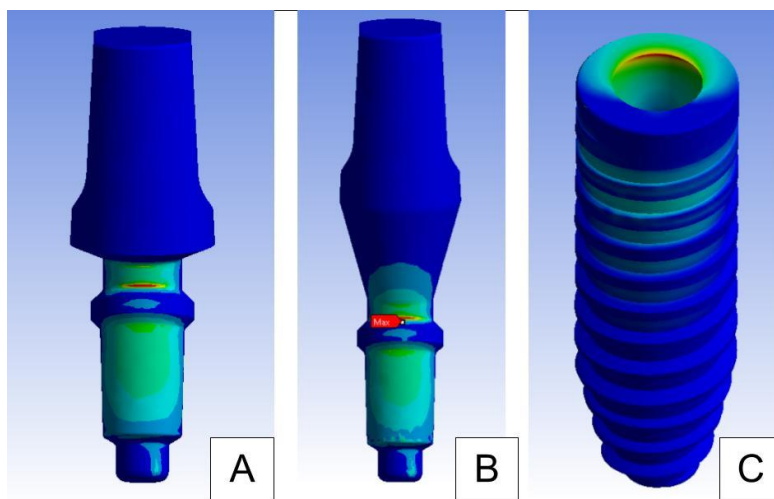


Figure I.4 – Representative images of the stress distribution: A – Abutment of WS group showing in the neck the maximum stress; B – Abutment of WL group showing same location of the maximum stress; C – Wide implant with stress concentration in the inner platform.

Discussion

The results of this study showed that the load-bearing capacity is reduced with the increase on transmucosal height of the abutment, however, the bending moment is improved with higher transmucosal height, rejecting the study hypothesis.

In Zirconia abutments (straight and 15-degree angulation) were tested at compressive strength testing. Higher fracture loads were reported for zirconia crowns in 4.5 mm implant platform. The fracture load values of straight and angulated abutments wasn't statistically significant (43).

two different abutment diameters and two transmucosal heights were used: 1) 4.5 x 2.5 mm; 2) 4.5 x 3.5 mm; 3) 3.3 x 2.5 mm; and 4) 3.3 x 3.5 mm, placed on indexed CM implants 3.5 mm in diameter x 13 mm in length. After the test, all abutments showed permanent deformation in the upper region and in the transmucosal portion, but without affecting the screw threads. Fractures were identified only in the 3.3mm diameter groups, while the 4.5 x 2.5mm abutment was the one with the best mechanical behavior and compressive strength (44).

In a study that compared the fatigue strength of the solid straight abutment (3.3 x 6 x 3.5mm) and the angled abutment with through screw (3.3 x 6 x 3.5mm, 17° of angulation) installed in implants CM bolts of 3.75 x 11mm (Neodent). Abutments were tested (26 specimens), 13 fractured below the five million established cycles, being 8 straight pillars and 5 five angled,

located predominantly at the height of the fourth thread of the prosthetic screw, which coincides with the internal thread of the CM component and the beginning of the space empty inside the set. However, there was no statistical difference in fracture resistance between abutments angled at 17° and straight abutments (36).

Another study compared straight abutments with different transmucosal heights, to see if there would be a difference in the loosening of the prosthetic abutment of 3.5x10 indexed CM implants (Unitite SIN). After torque application the abutments with transmucosal heights of 0.8, 3.5 and 5.5 mm were cycled and the detorque values of the abutments were measured. As a result, higher torque values were found for the 0.8 and 3.5 abutments, in contrast, the lowest values were found for the 5.5mm height abutments. However, no statistical difference was found between the three groups (24).

Different abutment angulations were tested 0°, 15° and 25th, according to neck height: 2 mm and 4 mm. Reverse torque values were measured in Ncm before and after cyclic loading, finding that, after mechanical cycling, the loosening of the prosthetic screw increases with increasing abutment angulation and height (45).

Referências

1. Imam AY, Yilmaz B, Özçelik TB, McGlumphy E. Salvaging an angled implant abutment with damaged internal threads: A clinical report. *J Prosthet Dent.* 2013;109(5):287–90.
2. Imam AY, Moshaverinia A, Chee WWL, McGlumphy EA. A technique for retrieving fractured implant screws. *J Prosthet Dent.* 2014;111(1):81–3.
3. Canpolat C, Özkurt-Kayahan Z, Kazazoğlu E. Management of a Fractured Implant Abutment Screw: A Clinical Report: Fractured Abutment Screw. *J Prosthodont.* 2014 Jul;23(5):402–5.
4. Yilmaz B, Mascarenhas F. Salvaging an implant with damaged internal threads. *J Prosthet Dent.* 2015;114(2):301–4.
5. Carneiro T de APN, Prudente MS, e Pessoa RS, Mendonça G, das Neves FD. A conservative approach to retrieve a fractured abutment screw – Case report. *J Prosthodont Res.* 2016 Apr;60(2):138–42.
6. Oh S-L, Barnes D. Managing a fractured implant: A clinical report. *J Prosthet Dent.* 2016 Apr;115(4):397–401.
7. Muroff FI. Removal and Replacement of a Fractured Dental Implant: Case Report: *Implant Dent.* 2003 Sep;12(3):206–10.
8. AL Quran FAM, Rashan BA, AL-Dwairi ZN. Management of Dental Implant Fractures. A Case History. *J Oral Implantol.* 2009 Aug;35(4):210–4.
9. Duraccio D, Mussano F, Faga MG. Biomaterials for dental implants: current and future trends. *J Mater Sci.* 2015 Jul;50(14):4779–812.

10. Pjetursson BE, Zarauz, C., Strasing, M., Sailer, I, Zwahlen, M., Zembic, A. A systematic review of the influence of the implant-abutment connection on the clinical outcomes of ceramic and metal implant abutments supporting fixed implant reconstructions. *Clin Oral Implants Res.* 2018;29(18):160–83.
11. Mittelstadt FG, Wiggers W, Cecato RC. Perfil técnico implante Arcsys [Internet]. DENTSCARE LTDA; 2016 [cited 2019 Mar 17]. Available from: https://issuu.com/fgmprodutosodontologicos/docs/arcsys_perfil_tecnico_final_rev01_v
12. Mangano F, Lucchina AG, Brucoli M, Migliario M, Mortellaro C, Mangano C. Prosthetic Complications Affecting Single-Tooth Morse-Taper Connection Implants: *J Craniofac Surg.* 2018 Mar;1.
13. Mangano C, Mangano F, Piattelli A, Iezzi G, Mangano A, La Colla L. Prospective clinical evaluation of 1920 Morse taper connection implants: results after 4 years of functional loading. *Clin Oral Implants Res.* 2009 Mar;20(3):254–61.
14. Mangano C, Mangano F, Shibli JA, Tettamanti L, Figliuzzi M, d’Avila S, et al. Prospective Evaluation of 2,549 Morse Taper Connection Implants: 1- to 6-Year Data. *J Periodontol.* 2011;82(1):52–61.
15. Mangano F, Macchi A, Caprioglio A, Sammons RL, Piattelli A, Mangano C. Survival and Complication Rates of Fixed Restorations Supported by Locking-Taper Implants: A Prospective Study with 1 to 10 Years of Follow-Up. *J Prosthodont.* 2014;23(6):434–44.
16. Mangano F, Shibli JA, Sammons RL, Veronesi G, Piattelli A, Mangano C. Clinical Outcome of Narrow-Diameter (3.3-mm) Locking-Taper Implants: A Prospective Study with 1 to

- 10 Years of Follow-up. *Int J Oral Maxillofac Implants*. 2014;29(2):448–55.
17. Mangano FG, Shibli JA, Sammons RL, Iaculli F, Piattelli A, Mangano C. Short (8-mm) locking-taper implants supporting single crowns in posterior region: a prospective clinical study with 1-to 10-years of follow-up. *Clin Oral Implants Res*. 2014;25(8):933–40.
 18. Mangano F, Frezzato I, Frezzato A, Veronesi G, Mortellaro C, Mangano C. The Effect of Crown-to-Implant Ratio on the Clinical Performance of Extra-Short Locking-Taper Implants: *J Craniofac Surg*. 2016 May;27(3):675–81.
 19. Demiralp KÖ, Akbulut N, Kursun S, Argun D, Bagis N, Orhan K. Survival Rate of Short, Locking Taper Implants with a Plateau Design: A 5-Year Retrospective Study. *BioMed Res Int [Internet]*. 2015 [cited 2019 Mar 28]; Available from: <https://www.hindawi.com/journals/bmri/2015/197451/>
 20. Geckili E, Geckili O, Bilhan H, Kutay O, Bilgin T. Clinical Comparison of Screw-Retained and Screwless Morse Taper Implant-Abutment Connections: One-year Postloading Results. *Int J Oral Maxillofac Implants*. 2017 Sep;32(5):1123–31.
 21. Mangano C, Luongo F, Mangano FG, Macchi A, Perrotti V, Piattelli A. Wide-diameter locking-taper implants: a prospective clinical study with 1 to 10-year follow-up. *J Osseointegration*. 2014 Jun 30;6(2):28–36.
 22. Urdaneta RA, Daher S, Leary J, Emanuel KM, Chuang S-K. The Survival of Ultrashort Locking-Taper Implants. 2012;12.

23. Bordin D, Cury AADB, Faot F. Influence of Abutment Collar Height and Implant Length on Stress Distribution in Single Crowns. *Braz Dent J.* 2019 Jun 3;30:238–43.
24. da Silva KRN, Joly JC, Peruzzo DC, Napimoga MH, Martinez EF. Influence of Transmucosal Height on Loss of Prosthetic Abutment Torque After Mechanical Cycling. *J Oral Implantol.* 2018 Jul 16;44(6):423–6.
25. Carpena ALM de M, Kinalski M, Bergoli CD, dos Santos MBF. Novel bendable abutments as a solution to correct unfavorable implant inclination. A clinical report. *J Esthet Restor Dent.* 2020 Dec;32(8):757–62.
26. Sordi MB, Apaza-Bedoya K, Cruz ACC, Volpato CAM, Benfatti CAM, Magini RS. Rehabilitation Challenge in Patient With High Smile Line: Case Report and Review of Surgical Protocols. *Clin Adv Periodontics.* 2020 Sep 25;cap.10122.
27. Sannino G, Barlattani A. Mechanical Evaluation of an Implant-Abutment Self-Locking Taper Connection: Finite Element Analysis and Experimental Tests. *Int J Oral Maxillofac Implants.* 2013;28(1):e17–26.
28. Markose J, Suresh S, Eshwar S, Rekha K, Jain V, Manvi S. Comparison of Platform Switched and Sloping Shoulder Implants on Stress Reduction in various Bone Densities: Finite Element Analysis. *J Contemp Dent Pract.* 2017 Jun 1;18(6):510–5.
29. de Souza Rendohl E, Brandt WC. Stress distribution with extra-short implants in an angled frictional system: A finite element analysis study. *J Prosthet Dent.* 2020 Dec;124(6):728.e1-728.e9.

30. International Organization for Standardization. ISO 14801:2007 Dentistry — Implants — Dynamic fatigue test for endosseous dental implants. Geneva, Switzerland; 2007.
31. Coppedê AR, Bersani E. Fracture Resistance of the Implant-Abutment Connection in Implants with Internal Hex and Internal Conical Connections Under Oblique Compressive Loading: An In Vitro Study. *Int J Prosthodont*. 2009;22(3):5.
32. Ka B de H, R AC, M A, Lr da SC, R PV. Biomechanical evaluation of anterior implants associated with titanium and zirconia abutments and monotype zirconia implants. *J Prosthodont Res*. 2020 Sep 9;65(1):73–7.
33. Chrcanovic BR, Kisch J, Albrektsson T, Wennerberg A. Factors influencing the fracture of dental implants. *Clin Implant Dent Relat Res*. 2018;20(1):58–67.
34. Merlo EG, Della Bona A, Griggs JA, Jodha KS, Corazza PH. Mechanical behavior and adhesive potential of glass fiber-reinforced resin-based composites for use as dentin analogues. *Am J Dent*. 2020 Dec;33(6):310–4.
35. Verplancke K, Waele WD, Bruyn HD. DENTAL IMPLANTS, WHAT SHOULD BE KNOWN BEFORE STARTING AN IN VITRO STUDY. 2011;10.
36. Santos VT de G, Trento CL, Santos PRS, Siqueira A dos S, Santos SV dos, Griza S. Análise da resistência à fratura entre pilares retos e angulados do sistema cone Morse. *Rev Odontol UNESP*. 2015 Apr;44(2):67–73.
37. Wu Y-L, Tsai M-H, Chen H-S, Chang Y-T, Lin T-T, Wu AY-J. Biomechanical effects of original equipment manufacturer and aftermarket abutment screws in zirconia abutment on dental implant assembly. *Sci Rep*. 2020 Dec;10(1):18406.

38. de la Rosa Castolo G, Guevara Perez SV, Arnoux P-J, Badih L, Bonnet F, Behr M. Mechanical strength and fracture point of a dental implant under certification conditions: A numerical approach by finite element analysis. *J Prosthet Dent.* 2018 Apr;119(4):611–9.
39. Chang H-C, Chang C-H, Li H-Y, Wang C-H. Biomechanical analysis of the press-fit effect in a conical Morse taper implant system by using an in vitro experimental test and finite element analysis. *J Prosthet Dent.* 2020 Dec;S0022391320306934.
40. Kawaguchi T, Kawata T, Kuriyagawa T, Sasaki K. In vivo 3-dimensional measurement of the force exerted on a tooth during clenching. *J Biomech.* 2007 Jan 1;40(2):244–51.
41. Proto Labs Titanium Grade 5 Ti-6Al-4V - DMLS [Internet]. [cited 2021 Jun 30]. Available from: <http://www.matweb.com/search/DataSheet.aspx?MatGUID=12529329832a4a0295dbf5451b8c4c75&ckck=1>
42. Medical Grade Stainless Steel 316LVM [Internet]. [cited 2021 Jun 30]. Available from: <http://www.matweb.com/search/DataSheet.aspx?MatGUID=29a84d10fada4e4fa3ebe3986e52d848>
43. Saker S, AL-Zordk W, Özcan M. Resistance to Fracture of Zirconia Abutments with Different Angulations: Impact of Implant Platform Diameter. *Eur J Dent.* 2020 Oct;14(04):517–24.
44. Lillo R, Parra C, Fuentes R, Borie E, Engelke W, Beltrán V. Compressive Resistance of Abutments with Different Diameters and Transmucosal Heights in Morse-Taper Implants. *Braz Dent J.* 2015 Apr;26(2):156–9.

45. El-Sheikh MAY, Mostafa TMN, El-Sheikh MM. Effect of different angulations and collar lengths of conical hybrid implant abutment on screw loosening after dynamic cyclic loading. *Int J Implant Dent* [Internet]. 2018 Dec [cited 2018 Dec 10];4(1). Available from: <https://journalimplantdent.springeropen.com/articles/10.1186/s40729-018-0149-z>

CONSIDERAÇÕES FINAIS

O presente estudo avaliou questões que ainda pairam na implantodontia, como utilização de implantes cone morse friccional, implantes estreitos, pilares angulados e utilização de diferentes alturas de transmucoso. Compreender desenhos de implantes e materiais utilizados é essencial para uma correta seleção dos melhores opções de tratamento e assim, permitir um melhor prognóstico das reabilitações com implantes dentários.

Sendo assim, a primeira hipótese de que diferentes configurações de implante e pilar não interfere na distribuição e magnitude de tensões, foi rejeitada, pois observou-se uma melhor distribuição das tensões conforme aumentou-se o diâmetro do implante, porém o aumento da altura de transmucoso aumentou o estresse máximo no pilar e reduziu no implante.

Com relação à segunda hipótese de que o diâmetro do implante não interfere na carga de fratura do sistema, foi rejeitada, pois com o aumento do diâmetro do implante observou-se diferença estatística entre os grupos na carga de fratura e no momento fletor.

Avaliando-se a terceira hipótese de que altura do transmucoso do componente não interfere na carga de fratura do sistema, foi rejeitada, pois com o aumento do transmucoso observou-se diferença estatística tanto na carga de fratura como no momento fletor.

Com relação à quarta hipótese de que o modo de falha seria similar entre as diferentes configurações implante e pilar, foi parcialmente rejeitada, pois os grupos com implante estreito e regular fraturaram de forma similar, porém o implante largo apresentou somente deformação. Enquanto isso, na avaliação da altura do transmucoso, observou-se deformação dos implantes dos dois grupos, porém somente no grupo de transmucoso de 2,5 mm todos os pilares deformaram, enquanto no grupo 5,5 mm somente 40% dos pilares deformaram.

REFERÊNCIAS

1. CFO A de C do. Cresce o número de implantes dentários no Brasil [Internet]. CFO. 2014 [cited 2021 Jun 15]. Available from: <https://website.cfo.org.br/cresce-o-numero-de-implantes-dentarios-no-brasil/>
2. Duraccio D, Mussano F, Faga MG. Biomaterials for dental implants: current and future trends. *J Mater Sci.* 2015 Jul;50(14):4779–812.
3. Pjetursson BE, Zarauz, C., Strasing, M., Sailer, I, Zwahlen, M., Zembic, A. A systematic review of the influence of the implant-abutment connection on the clinical outcomes of ceramic and metal implant abutments supporting fixed implant reconstructions. *Clin Oral Implants Res.* 2018;29(18):160–83.
4. Coelho PG, Granjeiro JM, Romanos GE, Suzuki M, Silva NRF, Cardaropoli G, et al. Basic research methods and current trends of dental implant surfaces. *J Biomed Mater Res B Appl Biomater.* 2009;88B(2):579–96.
5. Gaviria L, Salcido JP, Guda T, Ong JL. Current trends in dental implants. *J Korean Assoc Oral Maxillofac Surg.* 2014;40(2):50.
6. Abraham CM. A Brief Historical Perspective on Dental Implants, Their Surface Coatings and Treatments. *Open Dent J.* 2014 May 16;8:50–5.

7. Barbosa TP, Naves MM, Menezes HHM, Pinto PHC, Mello JDB, Costa HL. Topography and surface energy of dental implants: a methodological approach. *J Braz Soc Mech Sci Eng.* 2017 Jan 3;6(39):1895–907.
8. Lee J-H, Frias V, Lee K-W, Wright RF. Effect of implant size and shape on implant success rates: A literature review. *J Prosthet Dent.* 2005;94(4):377–81.
9. Schmitt CM, Nogueira-Filho G, Tenenbaum HC, Lai JY, Brito C, Döring H, et al. Performance of conical abutment (Morse Taper) connection implants: A systematic review: Performance of Conical Implant-Abutment Connection Systems. *J Biomed Mater Res A.* 2014 Feb;102(2):552–74.
10. Varise CG, Abi-Rached FO, Messias AM, Das Neves FD, Segalla JCM, Reis JMDSN. Sistema Cone Morse e utilização de pilares com plataforma switching. *Rev Bras Odontol.* 2015 Jan 4;72(1/2):56–61.
11. Caricasulo R, Malchiodi L, Ghensi P, Fantozzi G, Cucchi A. The influence of implant-abutment connection to peri-implant bone loss: A systematic review and meta-analysis. *Clin Implant Dent Relat Res.* 2018 Aug;20(4):653–64.
12. Vargas LCM, de Almeida EO, Rocha EP, Kina S, Anchieta RB, Júnior ACF, et al. Regular and Switching Platform: Bone Stress Analysis With Varying Implant Diameter. *J Oral Implantol.* 2013 Jun;39(3):326–31.
13. Liu S, Tang C, Yu J, Dai W, Bao Y, Hu D. The effect of platform switching on stress distribution in implants and periimplant bone studied by nonlinear finite element analysis. *J Prosthet Dent.* 2014;112(5):1111–8.
14. Freitas G, Hirata R, Bonfante E, Tovar N, Coelho P. Survival Probability of Narrow and Standard-Diameter Implants with

- Different Implant-Abutment Connection Designs. *Int J Prosthodont.* 2016 Feb;29(2):179–85.
15. Tsuruta K, Ayukawa Y, Matsuzaki T, Kihara M, Koyano K. The influence of implant–abutment connection on the screw loosening and microleakage. *Int J Implant Dent* [Internet]. 2018 Dec [cited 2018 Oct 10];4(1). Available from: <https://journalimplantdent.springeropen.com/articles/10.1186/s40729-018-0121-y>
 16. Rodrigues EDS, Benetti P, Carli JPD, Paranhos LR, Santos PL, Linden MS. A Comparison of Torque Stress on Abutment Screw of External Hexagon and Morse Taper Implant. *J Contemp Dent Pract.* 2018 Nov 1;19(11):1306–11.
 17. Ribeiro CG, Maia MLC, Scherrer SS, Cardoso AC, Wiskott HWA. Resistance of three implant-abutment interfaces to fatigue testing. *J Appl Oral Sci Rev FOB.* 2011 Aug;19(4):413–20.
 18. Seol H-W, Heo S-J, Koak J-Y, Kim S-K, Han C-H. Effect of cyclic loading on axial displacement of abutment into implant with internal tapered connection: a pilot study. *J Korean Acad Prosthodont.* 2013;51(4):315.
 19. Chrcanovic BR, Kisch J, Albrektsson T, Wennerberg A. Factors influencing the fracture of dental implants. *Clin Implant Dent Relat Res.* 2018;20(1):58–67.
 20. Singh A, Singh A, Vivek R, Chaturvedi TP, Chauhan P, Gupta S. SEM Analysis and Management of Fracture Dental Implant. *Case Rep Dent.* 2013;2013:270385.
 21. Lee J-H, Lee J-B, Kim M-Y, Yoon J-H, Choi S-H, Kim Y-T. Mechanical and biological complication rates of the modified lateral-screw-retained implant prosthesis in the posterior

- region: an alternative to the conventional Implant prosthetic system. *J Adv Prosthodont.* 2016 Apr;8(2):150–7.
22. Imam AY, Yilmaz B, Özçelik TB, McGlumphy E. Salvaging an angled implant abutment with damaged internal threads: A clinical report. *J Prosthet Dent.* 2013;109(5):287–90.
 23. Imam AY, Moshaverinia A, Chee WWL, McGlumphy EA. A technique for retrieving fractured implant screws. *J Prosthet Dent.* 2014;111(1):81–3.
 24. Canpolat C, Özkurt-Kayahan Z, Kazazoğlu E. Management of a Fractured Implant Abutment Screw: A Clinical Report: Fractured Abutment Screw. *J Prosthodont.* 2014 Jul;23(5):402–5.
 25. Yilmaz B, Mascarenhas F. Salvaging an implant with damaged internal threads. *J Prosthet Dent.* 2015;114(2):301–4.
 26. Carneiro T de APN, Prudente MS, e Pessoa RS, Mendonça G, das Neves FD. A conservative approach to retrieve a fractured abutment screw – Case report. *J Prosthodont Res.* 2016 Apr;60(2):138–42.
 27. Oh S-L, Barnes D. Managing a fractured implant: A clinical report. *J Prosthet Dent.* 2016 Apr;115(4):397–401.
 28. Muroff FI. Removal and Replacement of a Fractured Dental Implant: Case Report: *Implant Dent.* 2003 Sep;12(3):206–10.
 29. AL Quran FAM, Rasha BA, AL-Dwairi ZN. Management of Dental Implant Fractures. A Case History. *J Oral Implantol.* 2009 Aug;35(4):210–4.
 30. Mittelstadt FG, Wiggers W, Cecato RC. Perfil técnico implante Arcsys [Internet]. DENTSCARE LTDA; 2016

[cited 2019 Mar 17]. Available from: https://issuu.com/fgmprodutosodontologicos/docs/arcsys_perfil_tecnico_final_rev01_v

31. Mangano F, Macchi A, Caprioglio A, Sammons RL, Piattelli A, Mangano C. Survival and Complication Rates of Fixed Restorations Supported by Locking-Taper Implants: A Prospective Study with 1 to 10 Years of Follow-Up. *J Prosthodont.* 2014;23(6):434–44.
32. Mangano F, Shibli JA, Sammons RL, Veronesi G, Piattelli A, Mangano C. Clinical Outcome of Narrow-Diameter (3.3-mm) Locking-Taper Implants: A Prospective Study with 1 to 10 Years of Follow-up. *Int J Oral Maxillofac Implants.* 2014;29(2):448–55.
33. Mangano FG, Shibli JA, Sammons RL, Iaculli F, Piattelli A, Mangano C. Short (8-mm) locking-taper implants supporting single crowns in posterior region: a prospective clinical study with 1-to 10-years of follow-up. *Clin Oral Implants Res.* 2014;25(8):933–40.
34. Mangano F, Frezzato I, Frezzato A, Veronesi G, Mortellaro C, Mangano C. The Effect of Crown-to-Implant Ratio on the Clinical Performance of Extra-Short Locking-Taper Implants: *J Craniofac Surg.* 2016 May;27(3):675–81.
35. Mangano C, Raes F, Lenzi C, Eccellente T, Ortolani M, Luongo G, et al. Immediate Loading of Single Implants: A 2-Year Prospective Multicenter Study. *Int J Periodontics Restorative Dent.* 2017 Feb;37(1):69–78.
36. Mangano F, Lucchina AG, Bruccoli M, Migliario M, Mortellaro C, Mangano C. Prosthetic Complications Affecting Single-Tooth Morse-Taper Connection Implants: *J Craniofac Surg.* 2018 Mar;1.

37. Geckili E, Geckili O, Bilhan H, Kutay O, Bilgin T. Clinical Comparison of Screw-Retained and Screwless Morse Taper Implant-Abutment Connections: One-year Postloading Results. *Int J Oral Maxillofac Implants*. 2017 Sep;32(5):1123–31.
38. Elani HW, Starr JR, Da Silva JD, Gallucci GO. Trends in Dental Implant Use in the U.S., 1999-2016, and Projections to 2026. *J Dent Res*. 2018 Dec;97(13):1424–30.
39. Tey VHS, Phillips R, Tan K. Five-year retrospective study on success, survival and incidence of complications of single crowns supported by dental implants. *Clin Oral Implants Res*. 2017 May;28(5):620–5.
40. Stoichkov B, Kirov D. Analysis of the causes of dental implant fracture: A retrospective clinical study. *Quintessence Int*. 2018 Mar 16;49(4):279–86.
41. Stoicănescu M, Buzamet E, Budei DV, Craciun V, Budei R, Cosnita M, et al. Possible Causes in Breaking of Dental Implants Research. *Mater Sci Forum*. 2017 Sep;907:104–18.
42. Bozkaya D, Müftü S. Mechanics of the tapered interference fit in dental implants. *J Biomech*. 2003 Nov;36(11):1649–58.
43. Ugurel CS, Steiner M, Isik-Ozkol G, Kutay O, Kern M. Mechanical resistance of screwless morse taper and screw-retained implant-abutment connections. *Clin Oral Implants Res*. 2013;26(2):137–42.
44. Mangano C, Mangano F, Piattelli A, Iezzi G, Mangano A, La Colla L. Prospective clinical evaluation of 1920 Morse taper connection implants: results after 4 years of functional loading. *Clin Oral Implants Res*. 2009 Mar;20(3):254–61.

45. Mangano C, Mangano F, Shibli JA, Tettamanti L, Figliuzzi M, d'Avila S, et al. Prospective Evaluation of 2,549 Morse Taper Connection Implants: 1- to 6-Year Data. *J Periodontol*. 2011;82(1):52–61.
46. Demiralp KÖ, Akbulut N, Kursun S, Argun D, Bagis N, Orhan K. Survival Rate of Short, Locking Taper Implants with a Plateau Design: A 5-Year Retrospective Study. *BioMed Res Int [Internet]*. 2015 [cited 2019 Mar 28]; Available from: <https://www.hindawi.com/journals/bmri/2015/197451/>
47. Mangano C, Luongo F, Mangano FG, Macchi A, Perrotti V, Piattelli A. Wide-diameter locking-taper implants: a prospective clinical study with 1 to 10-year follow-up. *J Osseointegration*. 2014 Jun 30;6(2):28–36.
48. Urdaneta RA, Daher S, Leary J, Emanuel KM, Chuang S-K. The Survival of Ultrashort Locking-Taper Implants. 2012;12.
49. Urdaneta RA, Rodriguez S, McNeil DC, Weed M, Chuang S-K. The effect of increased crown-to-implant ratio on single-tooth locking-taper implants. *Int J Oral Maxillofac Implants*. 2010 Jul 1;25(4):729–43.
50. Petris GP, De Carli JP, Paranhos LR, Santos PL, Benetti P, Walber M, et al. Morse taper performance: A finite element analysis study. *Clinics [Internet]*. 2019 Mar 25 [cited 2021 Jun 20];74. Available from: <https://www.scielo.br/j/clin/a/YnmswGQRbJRcTBVthVDpNGs/?lang=en>
51. de la Rosa Castolo G, Guevara Perez SV, Arnoux P-J, Badih L, Bonnet F, Behr M. Mechanical strength and fracture point of a dental implant under certification conditions: A numerical approach by finite element analysis. *J Prosthet Dent*. 2018 Apr;119(4):611–9.

52. Erdemir A, Guess TM, Halloran J, Tadepalli SC, Morrison TM. Considerations for reporting finite element analysis studies in biomechanics. *J Biomech.* 2012 Feb;45(4):625–33.
53. Chang H-C, Chang C-H, Li H-Y, Wang C-H. Biomechanical analysis of the press-fit effect in a conical Morse taper implant system by using an in vitro experimental test and finite element analysis. *J Prosthet Dent.* 2020 Dec;S0022391320306934.
54. Merlo EG, Della Bona A, Griggs JA, Jodha KS, Corazza PH. Mechanical behavior and adhesive potential of glass fiber-reinforced resin-based composites for use as dentin analogues. *Am J Dent.* 2020 Dec;33(6):310–4.
55. Verplancke K, Waele WD, Bruyn HD. DENTAL IMPLANTS, WHAT SHOULD BE KNOWN BEFORE STARTING AN IN VITRO STUDY. 2011;10.
56. International Organization for Standardization. ISO 14801:2007 Dentistry — Implants — Dynamic fatigue test for endosseous dental implants. Geneva, Switzerland; 2007.
57. Santos VT de G, Trento CL, Santos PRS, Siqueira A dos S, Santos SV dos, Griza S. Análise da resistência à fratura entre pilares retos e angulados do sistema cone Morse. *Rev Odontol UNESP.* 2015 Apr;44(2):67–73.
58. Wu Y-L, Tsai M-H, Chen H-S, Chang Y-T, Lin T-T, Wu AY-J. Biomechanical effects of original equipment manufacturer and aftermarket abutment screws in zirconia abutment on dental implant assembly. *Sci Rep.* 2020 Dec;10(1):18406.
59. de Souza Rendohl E, Brandt WC. Stress distribution with extra-short implants in an angled frictional system: A finite

- element analysis study. *J Prosthet Dent.* 2020 Dec;124(6):728.e1-728.e9.
60. Chang H-C, Li H-Y, Chen Y-N, Chang C-H, Wang C-H. Mechanical analysis of a dental implant system under 3 contact conditions and with 2 mechanical factors. *J Prosthet Dent.* 2019 Oct;122(4):376–82.
 61. Kawaguchi T, Kawata T, Kuriyagawa T, Sasaki K. In vivo 3-dimensional measurement of the force exerted on a tooth during clenching. *J Biomech.* 2007 Jan 1;40(2):244–51.
 62. Proto Labs Titanium Grade 5 Ti-6Al-4V - DMLS [Internet]. [cited 2021 Jun 30]. Available from: <http://www.matweb.com/search/DataSheet.aspx?MatGUID=12529329832a4a0295dbf5451b8c4c75&ckck=1>
 63. Medical Grade Stainless Steel 316LVM [Internet]. [cited 2021 Jun 30]. Available from: <http://www.matweb.com/search/DataSheet.aspx?MatGUID=29a84d10fada4e4fa3ebe3986e52d848>
 64. Saker S, AL-Zordk W, Özcan M. Resistance to Fracture of Zirconia Abutments with Different Angulations: Impact of Implant Platform Diameter. *Eur J Dent.* 2020 Oct;14(04):517–24.
 65. Song S-Y, Lee J-Y, Shin S-W. Effect of Implant Diameter on Fatigue Strength. *Implant Dent.* 2017 Feb;26(1):59–65.
 66. Pellizzer EP, Verri FR, Falcón-Antenucci RM, Júnior JFS, de Carvalho PSP, de Moraes SLD, et al. Stress Analysis in Platform-Switching Implants: A 3-Dimensional Finite Element Study. *J Oral Implantol.* 2012 Oct 20;38(5):587–94.
 67. Moraes SLD de, Verri FR, Santiago Júnior JF, Almeida DA de F, Lemos CAA, Gomes JM de L, et al. Three-Dimensional

- Finite Element Analysis of Varying Diameter and Connection Type in Implants with High Crown-Implant Ratio. *Braz Dent J.* 2018 Feb;29(1):36–42.
68. Sannino G, Barlattani A. Mechanical Evaluation of an Implant-Abutment Self-Locking Taper Connection: Finite Element Analysis and Experimental Tests. *Int J Oral Maxillofac Implants.* 2013;28(1):e17–26.
 69. Markose J, Suresh S, Eshwar S, Rekha K, Jain V, Manvi S. Comparison of Platform Switched and Sloping Shoulder Implants on Stress Reduction in various Bone Densities: Finite Element Analysis. *J Contemp Dent Pract.* 2017 Jun 1;18(6):510–5.
 70. Nishigawa K, Bando E, Nakano M. Quantitative study of bite force during sleep associated bruxism. *J Oral Rehabil.* 2001 May;28(5):485–91.
 71. Bordin D, Cury AADB, Faot F. Influence of Abutment Collar Height and Implant Length on Stress Distribution in Single Crowns. *Braz Dent J.* 2019 Jun 3;30:238–43.
 72. da Silva KRN, Joly JC, Peruzzo DC, Napimoga MH, Martinez EF. Influence of Transmucosal Height on Loss of Prosthetic Abutment Torque After Mechanical Cycling. *J Oral Implantol.* 2018 Jul 16;44(6):423–6.
 73. Carpena ALM de M, Kinalski M, Bergoli CD, dos Santos MBF. Novel bendable abutments as a solution to correct unfavorable implant inclination. A clinical report. *J Esthet Restor Dent.* 2020 Dec;32(8):757–62.
 74. Sordi MB, Apaza-Bedoya K, Cruz ACC, Volpato CAM, Benfatti CAM, Magini RS. Rehabilitation Challenge in Patient With High Smile Line: Case Report and Review of

Surgical Protocols. Clin Adv Periodontics. 2020 Sep 25;cap.10122.

75. Coppedê AR, Bersani E. Fracture Resistance of the Implant-Abutment Connection in Implants with Internal Hex and Internal Conical Connections Under Oblique Compressive Loading: An In Vitro Study. Int J Prosthodont. 2009;22(3):5.
76. Ka B de H, R AC, M A, Lr da SC, R PV. Biomechanical evaluation of anterior implants associated with titanium and zirconia abutments and monotype zirconia implants. J Prosthodont Res. 2020 Sep 9;65(1):73–7.

